Published by
NIGERIAN SOCIETY OF PHYSICAL SCIENCES
Available online @ https://asr.nsps.org.ng/index.php/asr

African Scientific Reports 5 (2026) 565

African Scientific Reports

A delay differential approach with sensitivity analysis for tuberculosis transmission and control

Abidah Amir[a], Awais Ahmad[b], Shah Zeb[c], Siti Ainor Mohd Yatim[c], Farah Aini Abdullah[a,d,*]

[a]School of Mathematical Sciences, Universiti Sains Malaysia, Minden, USM 11800, Penang, Malaysia
[b]Department of Mathematics, Government College University Faisalabad, 38000, Pakistan
[c]School of Distance Education, Universiti Sains Malaysia, Minden, USM 11800, Penang, Malaysia
[d]Nonlinear Dynamics Research Center (NDRC), Ajman University, Ajman, United Arab Emirates

Abstract

Tuberculosis (TB) is considered a severe disease and remains a serious public health problem in developing regions, especially in Khyber Pakhtunkhwa (KPK), Pakistan, where the failure to timely diagnose the disease, poor access to healthcare, poverty, and treatment interruptions significantly contribute to the disease's transmission and persistence. The main goal of this research is to investigate the transmission and control dynamics of TB using a nonlinear delayed compartmental mathematical model, with particular interest in the surge of TB in the KPK region. In view of the rising burden of TB in the region, this study proposes a nonlinear delayed compartmental mathematical model of the spread behavior of TB. The proposed model includes two biologically relevant time delays, those of latent disease progression and treatment monitoring mechanisms. The qualitative analysis of the model is rigorously investigated. The basic mathematical properties, including positivity, boundedness, and existence of solutions, are established. The threshold dynamics of the disease is determined by the basic reproduction number $\mathcal{R}_0$, which is computed by the next-generation matrix method, and the disease-free equilibrium (DFE) and endemic equilibrium (EE) points are derived. Moreover, the stability of the equilibrium states is examined by using Lyapunov techniques and stability theory both locally and globally. A sensitivity analysis is conducted to determine the most important epidemiological parameters defining the spread of TB. The results obtained reveal that low values of $\mathcal{R}_0$ are obtained when the transmission-associated parameters are low, whereas high values associated with treatment efficiency and the delay associated with the control mechanism lead to low transmission of the disease. In particular, it is shown that the presence of the second delay parameter related to the supervised treatment and monitoring shows a significant decrease in the effective $\mathcal{R}_0$, thus highlighting the need for continuous treatment monitoring and patient follow-up programs. Numerical simulation is carried out using the nonstandard finite difference (NSFD) method to validate the theoretical results. The NSFD scheme is able to maintain mathematical consistency of the model solutions for all the selected step sizes, leading to stable numerical behavior. The results of the simulations are also consistent with the DFE being achieved for $\mathcal{R}_0 < 1$ and the persistence of the disease for $\mathcal{R}_0 > 1$. This study's findings highlight the importance of early diagnosis, successful supervision of treatment, controlled drug utilization and ongoing patient monitoring to significantly reduce TB transmission in KPK, Pakistan. The delayed tuberculosis model might be helpful for designing more effective disease control and intervention strategies by healthcare authorities and policymakers. Moreover, this work advances biomathematical modeling by merging the incorporation of biologically relevant time lags and the use of rigorous stability, sensitivity and dynamically consistent numerical simulations in a coherent framework for modeling infectious diseases.

DOI: 10.46481/asr.2026.5.2.565

Keywords: Tuberculosis, Basic reproduction number, Sensitivity analysis, Time-delay model, Infectious disease modeling

Article History:
Received: 01 June 2026
Received in revised form: 10 July 2026
Accepted for publication: 14 July 2026
Available online: 12 August 2026

*Corresponding Author Tel. No.: +60164437864.
Email address: farahaini@usm.my (Farah Aini Abdullah)

1. Introduction

A bacillus mycobacterium causes tuberculosis (TB), a disease that is mostly transmitted by aerosol, from an infected individual to those in close proximity through coughing, sneezing, spitting, or talking [1, 2]. TB is one of the top ten leading causes of death worldwide and continues to be one of the biggest public health issues, especially in developing nations. After HIV/AIDS, it is the second deadliest infectious disease brought on by a single infectious agent [3]. Over 60% of the global TB burden is attributed to developing nations where access to TB diagnosis and treatment is challenging [4]. Pakistan is one of them where this disease seriously threatens public health. Every year, health authorities report approximately 500,000 new cases of TB, resulting in the deaths of around 70,000 individuals [5]. Due to the high prevalence of multi drug resistant TB infections, Pakistan has the fifth-highest TB case burden in the world [6]. The northwest Pakistani province of KPK reports over fifty five thousands new individuals of TB of all kinds every year. In KPK province, about 462,920 TB cases were documented between 2002 and 2017 [1]. A number of epidemiological studies of TB have already been carried out in various districts of KPK [7]. These studies were undertaken on the epidemiology and risk factors analysis of TB in a particular district [8]. Global socioeconomic disparities, significant levels of population mobility, fast urbanization, and population increase are important structural factors of TB spread. Key social determinants of TB, including malnutrition and environmental conditions, as well as, financial and geographic impediments to healthcare access, are distributed unevenly as a result of these situations. One of the main risk factors for TB is these social determinants [9]. For example, poor ventilation and overcrowding in homes, workplaces, and communities increase the likelihood of uninfected individuals being exposed to TB infection [10]. Poverty can make people more vulnerable to illness and the severity of clinical results [11]. People who have TB symptoms frequently encounter major obstacles that prevent them from contacting health systems where a proper diagnosis could be arranged. These obstacles include challenges to medical availability of facilities [12], fear of being stigmatized if they seek disease diagnosis, and to get care when they become ill [13]. While the use of a patient's social network to enhance treatment adherence has been pioneered by DOTS (directly observed treatment, shortcourse), a social determinants framework also emphasizes how poverty-driven pessimism may contribute to high rates of treatment that compromise TB control [14].

Mathematical models are thought to be powerful and helpful tools for precisely predicting a disease's dynamic behavior and provide guidance on how to create effective control techniques [15–17]. Numerous models have been examined in the literature to learn more about the dynamics of TB in various parts of the world. In 1962, Waaler et al.[18] established the first mathematical model of TB based on three distinct demographic classifications. The system of nonlinear ODEs was then used by researchers Revelle et al.[19] to create a TB transmission model in 1967. Feng and Castillo-Chavez [20] created three distinct TB models and performed a detailed stability analysis with the help of model's fundamental $\mathcal{R}_0$. Another team of researchers Yang et al. [21] investigated the global dynamics of two TB models with inadequate therapy. In order to investigate TB transmission in endemic areas of the Asia, Trauer et al. [22] devised a mathematical model. Zhang et al. [23] put up a novel TB model and offered a plausible explanation for the actual TB cases in China. In order to eradicate TB in Philippine, one of the team of researchers Kim et al. [24] developed a model with efficient intervention techniques. Control strategies for reducing TB have also been suggested using the optimal control framework. In a two-strain TB model, Jung et al. [25] proposed the best control methods. It was the first study to use optimal control theory in a model of tuberculosis transmission. For the Republic of Korea, Whang et al. [26] created a mathematical TB model and recommended the best TB intervention techniques. By contrasting the government's TB budget with the best control outcomes, Choi and Jung also suggested a workable intervention strategy (Choi et al. [27]). A mathematical model for the dynamics of TB in the Philippines was created by Villasin et al. [28], taking into account BCG vaccination and calculating parameters from the available data.

A model to analyze the proportion of several scenarios of TB disease transmission with partial treatment was introduced by Yang et al. [21]. To investigate TB's global stability outcomes and the impact of heterogeneity on TB dispersion, a number of studies provided mathematical models for the disease [29]. Hospitalized and non-hospitalized infectious classes were included in the dynamic problem of TB disease that Zhang et al. [30] examined. Robert examined a mathematical model of TB in order to examine the effects of degradation and reinfection [23]. Additionally, a model for TB disease was presented by Egonmwan et al. [31] to assess the impact of treatment and analysis for infectious individuals. A number of fractional order and non-local derivatives that conclude the reduction of an integer-order derivative have recently been proposed by numerous scholars. For example, the theory of fractional derivative is introduced by Riemann-Liouville, and Caputo has made additional improvements. These kinds of operators are unworkable for the dynamical mathematical models, according to the notion of fractional derivatives singularity. Another researcher, Caputo-Fabrizio (CF) [32], suggested a unique derivative that uses the exponential function as its kernel to control these issues. In order to comprehend the CF nomenclature, we include a few applications; for more information, see [33]. The literature introduced a novel idea in which the kernel was transformed from non-local singular to non-local and non-singular. The representation of vanishing memory and clearly defined memory of the system being studied is the benefit of this new kernel. A new derivative that extended the Mittag-Leffler function to non-local and non-singular functions was created in 2016 by Atangana and Baleanu [34]. This recently developed derivative has been used in a variety of domains to describe real-world issues mathematically [35]. As a result, the majority of researchers are eager to learn more about the biology model of infectious disease. Some model researchers are concerned about the model's stability and optimization; see [36]. Creating a computational framework to solve a

mathematical model of streptococcus pneumonia infection with accuracy [37]. As a result a boundedness-preserving numerical model with immunization [38]. A novel mathematical model of the tuberculosis pandemic under the influence of consciousness [39]. The literature presents a fresh concept regarding numerical simulations and the optimal existence of a fractional order computer virus epidemic model [40].

In recent years, mathematical modelling of TB transmission has been much discussed because of the ongoing burden of TB, especially in developing regions like KPK, Pakistan. The present study is an extension of a previous TB model with two biologically meaningful time delays in the disease transmission process. In the previously published model [1], spread behavior were examined without considering the explicit delay effects which restricted the model's ability to account for realistic epidemiological processes involved in TB progression and treatment. The proposed model, on the other hand, adds a first delay parameter, τ_1, which describes the latent and delayed activation of TB infection, as well as a second delay parameter, τ_2, which describes the process of supervised treatment, medication adherence, patient follow-up, and controlled recovery. These two delays give a more realistic representation of TB natural history and enable a detailed examination of the effect of these delays on the dynamics of disease transmission. The analysis shows that the second delay has a significant impact on reducing the effective disease transmission and the $\mathcal{R}_0$ even if the first delay is decreased, indicating that monitoring treatment and healthcare intervention strategies will play a significant role in controlling TB transmission. Additionally, the extended model comes with a detailed sensitivity analysis to pinpoint the most important epidemiological parameters that could impact disease persistence and management. Numerical simulations are carried out with the NSFD scheme to maintain positivity, boundedness and dynamism of the solutions. The NSFD method yields stable and convergent solution which accurately represents theoretical properties of the continuous model, unlike the conventional numerical method. Thus, the use of dual time delays and sensitivity analysis and dynamically consistent numerical simulations gives a great improvement over the earlier developed model that gives valuable insight into the biological aspect of tuberculosis control and prevention strategies in KPK, Pakistan.

The rest of this paper is organized as follows: In the introduction of Section 1, TB is introduced, and the epidemiological importance of the disease in the KPK province, Pakistan, is highlighted. In addition, a review of the mathematical modeling methods that can be applied to the understanding of the spread behavior of TB is provided.The introduction of Section 1 introduces TB and its epidemiological importance in the province of KPK, Pakistan, and reviews some of the mathematical modeling approaches that have been used in the study of TB spread behavior. The details of the proposed delayed TB model by delay differential equation (DDEs) are given in Section 2, along with the biological assumptions and parameter descriptions. The qualitative properties of this model, such as positivity, boundedness, existence of solutions, disease-free and EE point, derivation of $\mathcal{R}_0$, and the local and global stability analysis of the equilibrium states, are also examined. The effect of the different epidemiological parameters on the $\mathcal{R}_0$ is studied in detail in Section 3, which is dedicated to sensitivity analysis. In addition, the biological interpretation of the first delay parameter is discussed to emphasize the epidemiological role of the parameter in the transmission and control of TB. In Section 4, numerical simulations are carried out with NSFD scheme. The positivity, boundedness, convergence and dynamical consistency of the numerical solutions are checked, and graphical results are given that support the theoretical results. In section 5, a modified model for TB with two biologically relevant time delays is introduced. The DFE, EE and $\mathcal{R}_0$ are derived and investigated for this extended model. Epidemiological aspects of both delays are also discussed, highlighting their involvement in the evolution of the disease and treatment monitoring. Lastly, in Section 6, the key analytical, biological, and numerical results are summarized and implications for TB control strategies in KPK, Pakistan, are discussed.

2. Methods and materials

2.1. Classes and parameters

To investigate the decline and rapid spread of TB, we propose an $SEITR$ transmission model with two latent classes. The total population is divided into six compartments: susceptible individuals $S(t)$, slow and fast latent classes $E_1(t)$ and $E_2(t)$, infected individuals $I(t)$, treated individuals $T(t)$, and recovered individuals $R(t)$. Following effective contact with an infected individual, a susceptible person enters either the slow latent class or the fast latent class, depending on the condition of the infected individual. Individuals in the slow latent class must first progress to the fast latent class before becoming infectious. The transitions among the compartments are illustrated in Figure 1. A proportion q $(0 < q < 1)$ of susceptible individuals enters the slow latent class E_1 after a time delay represented by $e^{-\mu\tau_1}$, while the remaining proportion $(1 - q)$ enters the fast latent class E_2 following successful contact with infected individuals. The model parameters are defined as follows: Λ denotes the recruitment (birth) rate, β the effective transmission rate, and μ the natural death rate across all compartments. Disease-induced death rates in the infected and treated classes are represented by σ_1 and σ_2, respectively. The parameters ϵ_1 and ϵ_2 denote the progression rates from E_1 to E_2 and from E_2 to I, respectively, while γ is the treatment rate of infected individuals. Individuals leave the treated class at rate δ, depending on the treatment stage. A proportion $\eta\delta T$ returns to the infected class I due to drug resistance, whereas the remaining proportion $(1 - \eta)\delta T$ returns to the slow latent class E_1. The recovery rate of treated patients is represented by the parameter α, and η $(0 < \eta < 1)$ denotes the proportion of treated individuals who develop drug resistance.

Table 1: Values of parameters and variables used in the SEITR TB model.

Parameter	Description	Value	Reference
Λ	Human birth ratio	450,862.20088	[1]
β	Human contact rate	0.6001	[1]
α	Recovery rate	0.0100	[1]
γ	Treatment rate	0.1500	[1]
μ	Natural death rate	1/67.7	[1]
σ_1	Disease-induced death rate in I	0.2738	[1]
σ_2	Disease-induced death rate during treatment process	0.1000	[1]
δ	Rate of leaving treatment of treated people and again entry to I or E_1	0.0649	[1]
η	Treatment failure rate	0.2959	[1]
ϵ_1	Transition rate from E_1 to E_2	0.2351	[1]
ϵ_2	Transfer rate from class E_2 to infected	0.2001	[1]
q	Ratio of susceptible individuals becoming infected	0.5259	[1]
τ_1	Time delay	≥ 0	Assumed
τ_2	Time delay	≥ 0	Assumed

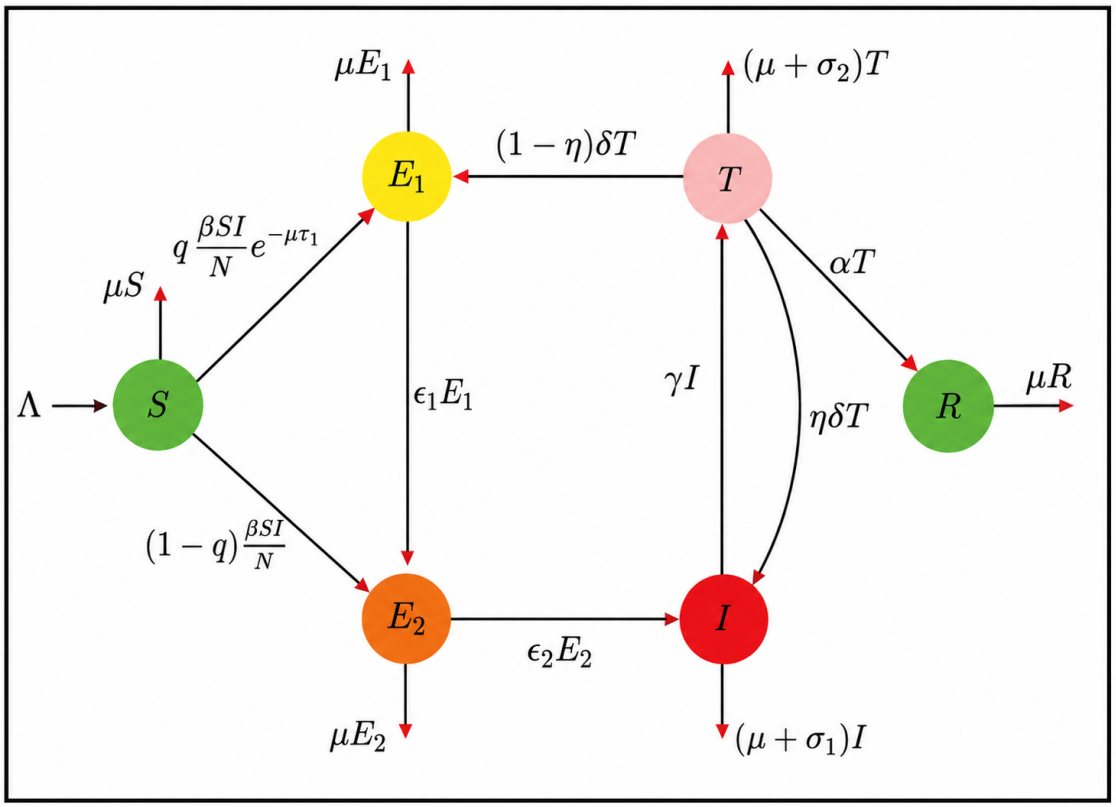

Figure 1: Delay in slow exposed.

2.2. *TB model with delay in the slow exposed class*

According to Figure 1, the initial modification of the TB model states that an infected person does not immediately become contagious. Instead, a susceptible person who is successfully infected by an infectious person first enters the slow and fast exposed class (E_1 and E_2), where the illness is latent for a while before becoming infectious (I). This is because TB infections have a protracted latent period. The values of all parameters are shown in Table 1.

An exponential delay factor ($e^{-\mu\tau_1}$) is added to the transmission from the susceptible class (S) to the exposed class (E_1) in order to account for this effect. This shows the likelihood of surviving the latent phase and the delay in the infection process. The delay between contracting an infection and being infectious is thus represented by the force of infection, which depends on the history of the infectious population. In the SE_1E_2ITR architecture, the delay term guarantees that the population moves naturally from one compartment to another ($S \rightarrow E_1 \rightarrow E_2 \rightarrow I \rightarrow T \rightarrow R$). People first become exposed (latent), and there is no direct passage from

the susceptible class to the infectious class. This modification enhances the model's realism and permits a deeper investigation of the dynamics of TB, particularly the influence of latency on disease transmission. The system of DDEs is

$$\frac{dS}{dt} = \Lambda - \frac{\beta e^{-\mu\tau_1} S(t-\tau) I(t-\tau)}{N} - \mu S(t), \tag{1}$$

$$\frac{dE_1}{dt} = q\frac{\beta e^{-\mu\tau_1} S(t-\tau) I(t-\tau)}{N} - (\mu + \epsilon_1) E_1(t) + (1-\eta)\delta T(t), \tag{2}$$

$$\frac{dE_2}{dt} = (1-q)\frac{\beta S(t) I(t)}{N} + \epsilon_1 E_1(t) - (\mu + \epsilon_2) E_2(t), \tag{3}$$

$$\frac{dI}{dt} = \epsilon_2 E_2(t) + \eta\delta T(t) - (\mu + \gamma + \sigma_1) I(t), \tag{4}$$

$$\frac{dT}{dt} = \gamma I(t) - (\mu + \delta + \sigma_2 + \alpha) T(t), \tag{5}$$

$$\frac{dR}{dt} = \alpha T(t) - \mu R(t). \tag{6}$$

Considering the starting conditions

$$S > 0, \;\; E_1 \geq 0, \;\; E_2 \geq 0, \;\; I \geq 0, \;\; T \geq 0, \;\; R \geq 0. \tag{7}$$

Here, t ≥ 0. $\tau \leq t$.
In order to simplify equations (1) to (6), let's indicate
$b_1 = \mu + \epsilon_1, \;\; b_2 = \mu + \epsilon_2, \;\; b_3 = \mu + \gamma + \sigma_1, \;\; b_4 = \mu + \delta + \sigma_2 + \alpha$

$$\frac{dS}{dt} = \Lambda - \frac{\beta e^{-\mu\tau_1} S I}{N} - \mu S, \tag{8}$$

$$\frac{dE_1}{dt} = q\frac{\beta e^{-\mu\tau_1} S I}{N} - b_1 E_1 + (1-\eta)\delta T, \tag{9}$$

$$\frac{dE_2}{dt} = (1-q)\frac{\beta S I}{N} + \epsilon_1 E_1 - b_2 E_2, \tag{10}$$

$$\frac{dI}{dt} = \epsilon_2 E_2 + \eta\delta T - b_3 I, \tag{11}$$

$$\frac{dT}{dt} = \gamma I - b_4 T, \tag{12}$$

$$\frac{dR}{dt} = \alpha T - \mu R. \tag{13}$$

2.3. Model analysis

The qualitative aspects of TB transmission are investigated by the suggested mathematical model. To comprehend the long-term dynamics of the disease, the system's basic characteristics such as the presence, boundedness, and stability of stable states are thoroughly investigated. This is crucial to ascertain whether control measures can be implemented and whether the disease will spread or deteriorate. Additionally, appropriate threshold parameters are computed to identify the conditions for the persistence and extinction of TB, much as the $\mathcal{R}_0$ in epidemiological systems. Because time delays account for both the latent phase of the disease and the interval between diagnosis and treatment responses, the model becomes more biologically realistic. As a result, the model provides a framework for comprehending the intricate relationships between susceptible, exposed, infected, and recovered persons as well as how intervention strategies impact the dynamics of the disease.

Theorem 2.1. The proposed disease model has a non-negative solution that provides nonnegative starting circumstances for any t ≥ 0.

Proof. Assume that the starting circumstances with initial conditions, examine the first equation:

$$\frac{dS}{dt} = \Lambda - \frac{\beta e^{-\mu\tau_1} S I}{N} - \mu S.$$

Since $I(t) \geq 0$, we have

$$\frac{\beta e^{-\mu\tau_1} I(t)}{N} \geq 0.$$

Thus,

$$\frac{dS}{dt} \geq -\left(\frac{\beta e^{-\mu\tau_1} I(t)}{N} + \mu\right) S(t).$$

Let

$$A(t) = \frac{\beta e^{-\mu\tau_1} I(t)}{N} + \mu.$$

Then,

$$\frac{dS}{dt} \geq -A(t)S(t).$$

Multiplying by integrating factor with both sides

$$\exp\left(\int_0^t A(s)\,ds\right),$$

we obtain

$$\frac{d}{dt}\left[S(t)\exp\left(\int_0^t A(s)\,ds\right)\right] \geq 0.$$

Integrating from 0 to t, we get

$$S(t)\exp\left(\int_0^t A(s)\,ds\right) \geq S(0).$$

Hence,

$$S(t) \geq S(0)\exp\left(-\int_0^t A(s)\,ds\right) > 0.$$

Likewise, in the case of the exposed class E_1,

$$\frac{dE_1}{dt} = q\frac{\beta e^{-\mu\tau_1} S I}{N} - b_1 E_1 + (1-\eta)\delta T.$$

All inflow terms are non-negative, so that it follows that

$$\frac{dE_1}{dt} \geq -b_1 E_1,$$

which implies

$$E_1(t) \geq E_1(0)e^{-b_1 t} > 0.$$

For E_2,

$$\frac{dE_2}{dt} = (1-q)\frac{\beta S I}{N} + \epsilon_1 E_1 - b_2 E_2.$$

Therefore,

$$\frac{dE_2}{dt} \geq -b_2 E_2,$$

and hence

$$E_2(t) \geq E_2(0)e^{-b_2 t} > 0.$$

For people infected with the virus,

$$\frac{dI}{dt} = \epsilon_2 E_2 + \eta\delta T - b_3 I.$$

Thus,

$$\frac{dI}{dt} \geq -b_3 I,$$

which gives

$$I(t) \geq I(0)e^{-b_3 t} > 0.$$

For the treatment class,

$$\frac{dT}{dt} = \gamma I - b_4 T.$$

Hence,

$$\frac{dT}{dt} \geq -b_4 T,$$

and therefore

$$T(t) \geq T(0)e^{-b_4 t} > 0.$$

Finally,

$$\frac{dR}{dt} = \alpha T - \mu R.$$

Thus,

$$\frac{dR}{dt} \geq -\mu R,$$

which implies

$$R(t) \geq R(0)e^{-\mu t} > 0.$$

It follows, then, that for all $t > 0$, all state variables are positive. □

Theorem 2.2. The solutions of the system are bounded in a feasible unique region $\Omega \subset \mathbb{R}^6_+$.

Proof. Let $N(t)$ is the sum of all classes and let the population at time t be the total population. Differentiating $N(t)$ with respect to time, we get

$$\begin{aligned}\frac{dN}{dt} = \Lambda - \frac{\beta e^{-\mu\tau_1} S I}{N} - \mu S + q\frac{\beta e^{-\mu\tau_1} S I}{N} - (\mu + \epsilon_1)E_1 + (1-\eta)\delta T \\ + (1-q)\frac{\beta S I}{N} + \epsilon_1 E_1 - (\mu + \epsilon_2)E_2 + \epsilon_2 E_2 + \eta\delta T - (\mu + \gamma + \sigma_1)I \\ + \gamma I - (\mu + \delta + \sigma_2 + \alpha)T + \alpha T - \mu R.\end{aligned}$$

After simplification, we get

$$\frac{dN}{dt} = \Lambda - \mu N - \sigma_1 I - \sigma_2 T.$$

Since $\sigma_1 I \geq 0$ and $\sigma_2 T \geq 0$, it follows that

$$\frac{dN}{dt} \leq \Lambda - \mu N.$$

Consider the differential equation

$$\frac{dN}{dt} = \Lambda - \mu N.$$

It has a solution of

$$N(t) = \frac{\Lambda}{\mu} + \left(N(0) - \frac{\Lambda}{\mu}\right)e^{-\mu t}.$$

Hence,

$$0 \leq N(t) \leq \frac{\Lambda}{\mu}, For\ any\ t \geq 0.$$

Hence the feasible region is

$$\Omega = \left\{(S, E_1, E_2, I, T, R) \in \mathbb{R}^6_+ : N(t) \leq \frac{\Lambda}{\mu}\right\}.$$

The following are therefore all the solutions that are uniformly bounded in Ω of the proposed TB model. □

2.4. Model equilibrium point

Absence and persistence of TB is defined by the presence and stability of the TB-free equilibrium and EE of the model proposed. The DFE is the point in which there is complete absence of TB in the community and it is achieved within the feasible region of the system. However, the EE occurs when the $\mathcal{R}_0$ is greater than one, meaning that the disease is ongoing and can be transmitted. These equilibrium states are important in the analysis of the qualitative behavior, stability properties and long-term dynamics of the model for the transmission of TB.

2.4.1. DFE point

The DFE points are:

$$\varepsilon_0 = (S_0, E_{10}, E_{20}, I_0, T_0, R_0) = \left(\frac{\Lambda}{\mu}, 0, 0, 0, 0, 0\right). \tag{14}$$

2.4.2. Reproduction number

The ($\mathcal{R}_0$) is among the most crucial threshold parameters in an epidemiological model. It decides if TB will remain or go extinct in a population. From a biological point of view, ($\mathcal{R}_0$) is the average number of secondary infections generated by an infectious person in the entire infectious period in a fully susceptible community. Hence it is an important tool in gaining insight of transmission and control of TB. The compartments $(E_1), (E_2), (I)$, and (T) in the proposed delayed SEITR TB model represent the infected classes, (S) represents the susceptible population and (R) represents the recovered population. We use the next-generation matrix method of van den Driessche and Watmough to calculate the $\mathcal{R}_0$. This approach gives a structured analysis of the transmission of infectious diseases. Let x be the vector of infected compartments, and y the vector of non-infected compartments [41]. The system can then be expressed in the form

$$\frac{dx}{dt} = F(x, y) - V(x, y),$$

where (F(x,y)) is the appearance of new infections, and (V(x,y)) is the movement of people between infected compartments due to progression, treatment, recovery, and natural death. The matrices (F) and (V) are the linearizations of the infected subsystem at the DFE. The next generation matrix theory says that the $\mathcal{R}_0$ is equal to the spectral radius of the matrix (FV^{-1}), or

$$\mathcal{R}_0 = (FV^{-1}).$$

The epidemiology of ($\mathcal{R}_0$) is known. If

$$\mathcal{R}_0 < 1,$$

Then, each infected person produces, on average, fewer than one new case of infection, and the disease slowly dies out of the population. For this case, the DFE is locally asymptotically stable (LAS). Were the other way, however,

$$\mathcal{R}_0 > 1,$$

Infection can invade the population and hold the disease, with the DFE being unstable. Moreover, the stability properties of the equilibrium points are very sensitive to the value of ($\mathcal{R}_0$). This can be checked with the Jacobian matrix computed at the DFE. Therefore, the matrices (F) and (V) of the infected subsystem is described as follows:

$$F = \begin{pmatrix} 0 & 0 & q\beta e^{-\mu\tau_1} & 0 \\ 0 & 0 & (1-q)\beta & 0 \\ 0 & 0 & 0 & 0 \\ 0 & 0 & 0 & 0 \end{pmatrix},$$

$$V = \begin{pmatrix} b_1 & 0 & 0 & -(1-\eta)\delta \\ -\epsilon_1 & b_2 & 0 & 0 \\ 0 & -\epsilon_2 & b_3 & -\eta\delta \\ 0 & 0 & -\gamma & b_4 \end{pmatrix},$$

$$FV^{-1} = \begin{pmatrix} \frac{q\beta e^{-\mu\tau_1}(1-\eta)\delta\gamma\epsilon_1}{\Delta} & \frac{q\beta e^{-\mu\tau_1}(1-\eta)\delta\gamma b_1}{\Delta} & \frac{q\beta e^{-\mu\tau_1} b_1 b_2 b_4}{\Delta} & \frac{q\beta e^{-\mu\tau_1}\delta b_1(\eta b_2 + (1-\eta)\epsilon_2)}{\Delta} \\ \frac{(1-q)\beta(1-\eta)\delta\gamma\epsilon_1}{\Delta} & \frac{(1-q)\beta(1-\eta)\delta\gamma b_1}{\Delta} & \frac{(1-q)\beta b_1 b_2 b_4}{\Delta} & \frac{(1-q)\beta\delta b_1(\eta b_2 + (1-\eta)\epsilon_2)}{\Delta} \\ 0 & 0 & 0 & 0 \\ 0 & 0 & 0 & 0 \end{pmatrix},$$

where

$$\Delta = b_1 b_2 b_3 b_4 - \eta\delta\gamma b_1 b_2 - (1-\eta)\delta\gamma\epsilon_1\epsilon_2.$$

Notice that the matrix FV^{-1} is rank one, and that the dominant eigenvalue is the non-zero characteristic root. Thus, the $\mathcal{R}_0$ is:

$$\mathcal{R}_0 = \rho(FV^{-1}),$$

Here, $\rho(FV^{-1})$ is the spectral radius of the matrix FV^{-1}. Hence, the $\mathcal{R}_0$ of the proposed TB model is

$$\mathcal{R}_0 = \frac{\beta\epsilon_2 b_4 \left[q\epsilon_1 e^{-\mu\tau_1} + (1-q)b_1\right]}{b_1 b_2 b_3 b_4 - \eta\delta\gamma b_1 b_2 - (1-\eta)\delta\gamma\epsilon_1\epsilon_2}. \tag{15}$$

2.4.3. EE point

The EE points are:

$$\varepsilon_1 = (S, E_1, E_2, I, T, R) = (S^*, E_1^*, E_2^*, I^*, T^*, R^*).$$

This implies that,

$$\left(\frac{\Lambda}{\mu + \dfrac{\beta e^{-\mu\tau_1} I^*}{N}},\ \frac{1}{b_1}\left(\frac{q\beta e^{-\mu\tau_1} S^* I^*}{N} + (1-\eta)\delta T^*\right),\ \frac{1}{b_2}\left(\frac{(1-q)\beta S^* I^*}{N} + \epsilon_1 E_1^*\right),\ \frac{\epsilon_2 E_2 + \eta\delta T}{b_3},\ \frac{\gamma I^*}{b_4},\ \frac{\alpha\gamma I^*}{\mu b_4} \right). \tag{16}$$

2.5. Stability analysis

This section looks at the system's stability at endemic and DFE, both LAS and GAS.

Theorem 2.3. The DFE point

$$\varepsilon_0 = \left(\frac{\Lambda}{\mu}, 0, 0, 0, 0, 0\right).$$

of the proposed delayed SEITR TB model is LAS if $\mathcal{R}_0 < 1$, and unstable if $\mathcal{R}_0 > 1$.

Proof. The system has the following Jacobian matrix:

$$J = \begin{pmatrix} -\dfrac{\beta e^{-\mu\tau_1} I}{N} - \mu & 0 & 0 & -\dfrac{\beta e^{-\mu\tau_1} S}{N} & 0 & 0 \\ \dfrac{q\beta e^{-\mu\tau_1} I}{N} & -b_1 & 0 & \dfrac{q\beta e^{-\mu\tau_1} S}{N} & (1-\eta)\delta & 0 \\ \dfrac{(1-q)\beta I}{N} & \epsilon_1 & -b_2 & \dfrac{(1-q)\beta S}{N} & 0 & 0 \\ 0 & 0 & \epsilon_2 & -b_3 & \eta\delta & 0 \\ 0 & 0 & 0 & \gamma & -b_4 & 0 \\ 0 & 0 & 0 & 0 & \alpha & -\mu \end{pmatrix}.$$

At the DFE point, calculating the matrix

$$\varepsilon_0 = \left(\frac{\Lambda}{\mu}, 0, 0, 0, 0, 0\right),$$

we obtain

$$J(\varepsilon_0) = \begin{pmatrix} -\mu & 0 & 0 & -\beta e^{-\mu\tau_1} & 0 & 0 \\ 0 & -b_1 & 0 & q\beta e^{-\mu\tau_1} & (1-\eta)\delta & 0 \\ 0 & \epsilon_1 & -b_2 & (1-q)\beta & 0 & 0 \\ 0 & 0 & \epsilon_2 & -b_3 & \eta\delta & 0 \\ 0 & 0 & 0 & \gamma & -b_4 & 0 \\ 0 & 0 & 0 & 0 & \alpha & -\mu \end{pmatrix}.$$

The characteristic equation is the same as the one below:

$$|J(\varepsilon_0) - \lambda I| = 0.$$

Obviously, the two eigenvalues are

$$\lambda_1 = -\mu, \qquad \lambda_2 = -\mu,$$

which are negative. The rest of the eigenvalues are calculated for the infected subsystem

$$\begin{pmatrix} -b_1 & 0 & q\beta e^{-\mu\tau_1} & (1-\eta)\delta \\ \epsilon_1 & -b_2 & (1-q)\beta & 0 \\ 0 & \epsilon_2 & -b_3 & \eta\delta \\ 0 & 0 & \gamma & -b_4 \end{pmatrix}.$$

The next-generation matrix approach gives rise to the associated $\mathcal{R}_0$.

$$\mathcal{R}_0 = \frac{\beta\epsilon_2 b_4 \left[q\epsilon_1 e^{-\mu\tau_1} + (1-q)b_1\right]}{b_1 b_2 b_3 b_4 - \eta\delta\gamma b_1 b_2 - (1-\eta)\delta\gamma\epsilon_1\epsilon_2}.$$

The characteristic polynomial of the infected subsystem is the expression: Routh-Hurwitz stability criterion. Therefore all of the eigenvalues are negative. If the following conditions apply, then both the real parts of them are:

$$d_1 > 0, \qquad d_2 > 0, \qquad d_3 > 0, \qquad d_4 > 0,$$

$$d_1 d_2 > d_3,$$

and

$$d_1 d_2 d_3 > d_1^2 d_4 + d_3^2.$$

The conditions given above are satisfied whenever, as can be seen by substituting the coefficients of the characteristic polynomial.

$$\mathcal{R}_0 < 1.$$

So, the DFE point ε_0 is LAS when

$$\mathcal{R}_0 < 1,$$

and unstable if

$$\mathcal{R}_0 > 1.$$

Hence the proof is finished. □

Theorem 2.4. When the population is not affected by the disease, it is known as the DFE point.

$$\varepsilon_0 = \left(\frac{\Lambda}{\mu}, 0, 0, 0, 0, 0\right)$$

The proposed delayed SEITR TB model is GAS for all delays, when

$$\mathcal{R}_0 < 1.$$

Proof. Construct the following Lyapunov function:

$$V(E_1, E_2, I, T) = E_1 + E_2 + c_1 I + c_2 T,$$

$c_1 > 0$ and $c_2 > 0$ are positive constants to be determined. Differentiate V with respect to the solutions of the system,

$$\frac{dV}{dt} = \frac{dE_1}{dt} + \frac{dE_2}{dt} + c_1\frac{dI}{dt} + c_2\frac{dT}{dt}.$$

By substituting the system equations, we get

$$\begin{aligned}\frac{dV}{dt} = {} & q\frac{\beta e^{-\mu\tau_1} S I}{N} - b_1 E_1 + (1-\eta)\delta T \\ & + (1-q)\frac{\beta S I}{N} + \epsilon_1 E_1 - b_2 E_2 \\ & + c_1\left(\epsilon_2 E_2 + \eta\delta T - b_3 I\right) \\ & + c_2\left(\gamma I - b_4 T\right).\end{aligned}$$

Rearranging terms gives

$$\begin{aligned}\frac{dV}{dt} = {} & \left(\epsilon_1 - b_1\right) E_1 + \left(c_1\epsilon_2 - b_2\right) E_2 \\ & + \left[q\beta e^{-\mu\tau_1} + (1-q)\beta - c_1 b_3 + c_2\gamma\right] I \\ & + \left[(1-\eta)\delta + c_1\eta\delta - c_2 b_4\right] T.\end{aligned}$$

With the correct choices of the constants c_1 and c_2, the above expression becomes.

$$\frac{dV}{dt} \leq (\mathcal{R}_0 - 1) I.$$

Therefore, if

$$\mathcal{R}_0 < 1,$$

then

$$\frac{dV}{dt} < 0,$$

for all

$$(E_1, E_2, I, T) \neq (0, 0, 0, 0).$$

$$\frac{dV}{dt} = 0$$

iff

$$E_1 = E_2 = I = T = 0.$$

In consequence, from the principle of invariance of LaSalle (LIP), the point of DFE is an invariant point.

$$\varepsilon_0 = \left(\frac{\Lambda}{\mu}, 0, 0, 0, 0, 0\right)$$

is GAS for all

$$\mathcal{R}_0 < 1.$$

Thus, this completes the proof. □

Theorem 2.5. The EE point

$$E^* = (S^*, E_1^*, E_2^*, I^*, T^*, R^*)$$

The proposed delayed SEITR TB model is GAS for all $t > 0$ if $\mathcal{R}_0 > 1$.

Proof. To prove GAS of the EE point, we will use the Lyapunov function

$$\begin{aligned} V = &\left(S - S^* - S^* \ln \frac{S}{S^*}\right) + \left(E_1 - E_1^* - E_1^* \ln \frac{E_1}{E_1^*}\right) \\ &+ \left(E_2 - E_2^* - E_2^* \ln \frac{E_2}{E_2^*}\right) + \left(I - I^* - I^* \ln \frac{I}{I^*}\right) \\ &+ \left(T - T^* - T^* \ln \frac{T}{T^*}\right) + \left(R - R^* - R^* \ln \frac{R}{R^*}\right). \end{aligned}$$

Taking the time derivative of V along the trajectories of the system gives

$$\begin{aligned} \frac{dV}{dt} = &\left(1 - \frac{S^*}{S}\right)\frac{dS}{dt} + \left(1 - \frac{E_1^*}{E_1}\right)\frac{dE_1}{dt} \\ &+ \left(1 - \frac{E_2^*}{E_2}\right)\frac{dE_2}{dt} + \left(1 - \frac{I^*}{I}\right)\frac{dI}{dt} \\ &+ \left(1 - \frac{T^*}{T}\right)\frac{dT}{dt} + \left(1 - \frac{R^*}{R}\right)\frac{dR}{dt}. \end{aligned}$$

Then, substituting in the model equations, we get

$$\begin{aligned} \frac{dV}{dt} = &\left(1 - \frac{S^*}{S}\right)\left(\Lambda - \frac{\beta e^{-\mu\tau_1} S I}{N} - \mu S\right) \\ &+ \left(1 - \frac{E_1^*}{E_1}\right)\left(q\frac{\beta e^{-\mu\tau_1} S I}{N} - b_1 E_1 + (1-\eta)\delta T\right) \\ &+ \left(1 - \frac{E_2^*}{E_2}\right)\left((1-q)\frac{\beta S I}{N} + \epsilon_1 E_1 - b_2 E_2\right) \\ &+ \left(1 - \frac{I^*}{I}\right)(\epsilon_2 E_2 + \eta\delta T - b_3 I) \\ &+ \left(1 - \frac{T^*}{T}\right)(\gamma I - b_4 T) \end{aligned}$$

$$+\left(1-\frac{R^*}{R}\right)(\alpha T-\mu R),$$

since

$$E^* = (S^*, E_1^*, E_2^*, I^*, T^*, R^*)$$

The point is an EE point, when we have

$$\frac{dS^*}{dt} = \frac{dE_1^*}{dt} = \frac{dE_2^*}{dt} = \frac{dI^*}{dt} = \frac{dT^*}{dt} = \frac{dR^*}{dt} = 0.$$

If the equilibrium relations are used and the above expression is simplified, then

$$\frac{dV}{dt} \leq 0,$$

for all

$$(S, E_1, E_2, I, T, R) \in \Omega,$$

where

$$\Omega = \left\{(S, E_1, E_2, I, T, R) \in \mathbb{R}_+^6 : N(t) \leq \frac{\Lambda}{\mu}\right\}$$

is bounded and positive invariant. Furthermore,

$$\frac{dV}{dt} = 0$$

iff

$$S = S^*, \quad E_1 = E_1^*, \quad E_2 = E_2^*, \quad I = I^*, \quad T = T^*, \quad R = R^*.$$

Thus, according to LIP, the EE point E^* is GAS when.

$$\mathcal{R}_0 > 1.$$

Hence, the proof is completed. □

3. Sensitivity analysis of parameters

To investigate how the $\mathcal{R}_0$ is affected by parameters of the model, sensitivity analysis is performed. This analysis is crucial in determining the parameters that are important to transmission and control of TB within the population. Additionally, it provides helpful information on which epidemiological aspects should be targeted in order to reduce the disease's spread. The sensitivity index for an epidemiological model is the ratio of the change in the $\mathcal{R}_0$ to a unit change in a parameter in that model. Therefore, it measures how much of a dependence the model's parameters have on $\mathcal{R}_0$. The sensitivity index of $\mathcal{R}_0$ with respect to any parameter P is given [42] by

$$\Upsilon_P^{\mathcal{R}_0} = \frac{\partial \mathcal{R}_0}{\partial P} \times \frac{P}{\mathcal{R}_0}.$$

If the sensitivity index is positive, the parameter is a factor that would increase the value of $\mathcal{R}_0$ if it increased, thus helping the spread of the disease. On the other hand, if the sensitivity index is negative, this suggests that, for an increase in the parameter, there is a decrease in $\mathcal{R}_0$, and this helps to control the disease. The sensitivity indices are calculated for the major epidemiological parameters in the proposed SEITR TB model, which are related to the transmission of TB, progression of the disease, treatment, recovery and delay effects. The following parameters have positive impact on the $\mathcal{R}_0$. Therefore, the more these parameters are increased, the more the disease spreads.

$$\frac{\partial \mathcal{R}_0}{\partial \beta} = \frac{\epsilon_2 b_4 \left[q\epsilon_1 e^{-\mu\tau_1} + (1-q)b_1\right]}{b_1 b_2 b_3 b_4 - \eta\delta\gamma b_1 b_2 - (1-\eta)\delta\gamma\epsilon_1\epsilon_2} > 0.$$

$$\frac{\partial \mathcal{R}_0}{\partial \epsilon_1} = \frac{\beta\epsilon_2 b_4 q e^{-\mu\tau_1}}{b_1 b_2 b_3 b_4 - \eta\delta\gamma b_1 b_2 - (1-\eta)\delta\gamma\epsilon_1\epsilon_2} > 0.$$

$$\frac{\partial \mathcal{R}_0}{\partial \epsilon_2} = \frac{\beta b_4 \left[q\epsilon_1 e^{-\mu\tau_1} + (1-q)b_1\right]}{b_1 b_2 b_3 b_4 - \eta\delta\gamma b_1 b_2 - (1-\eta)\delta\gamma\epsilon_1\epsilon_2} > 0.$$

$$\frac{\partial \mathcal{R}_0}{\partial \delta} = \frac{\beta\epsilon_2 b_4 \left[q\epsilon_1 e^{-\mu\tau_1} + (1-q)b_1\right]\gamma\left(\eta b_1 b_2 + (1-\eta)\epsilon_1\epsilon_2\right)}{\left(b_1 b_2 b_3 b_4 - \eta\delta\gamma b_1 b_2 - (1-\eta)\delta\gamma\epsilon_1\epsilon_2\right)^2} > 0.$$

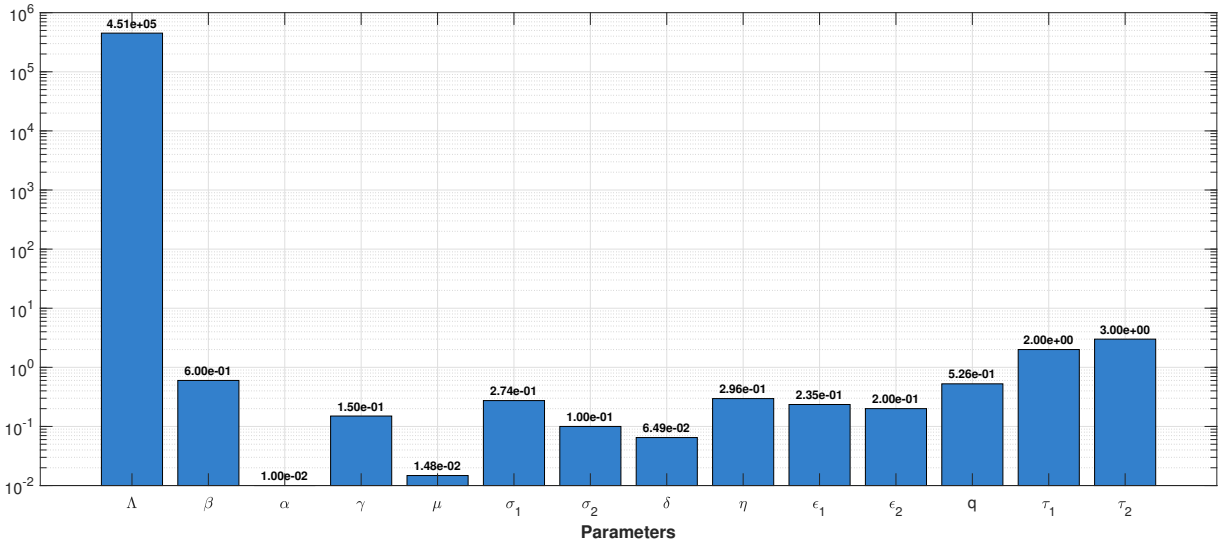

Figure 2: Parameter values.

The next set of parameters negatively affect the $\mathcal{R}_0$ $\mathcal{R}_0$. So, raising these parameters will help to decrease transmission of TB.

$$\frac{\partial \mathcal{R}_0}{\partial \gamma} = -\frac{\beta\epsilon_2 b_4 \left[q\epsilon_1 e^{-\mu\tau_1} + (1-q)b_1\right]\delta\left(\eta b_1 b_2 + (1-\eta)\epsilon_1\epsilon_2\right)}{\left(b_1 b_2 b_3 b_4 - \eta\delta\gamma b_1 b_2 - (1-\eta)\delta\gamma\epsilon_1\epsilon_2\right)^2} < 0.$$

$$\frac{\partial \mathcal{R}_0}{\partial \mu} = -\frac{\beta\epsilon_2 b_4 \left[q\epsilon_1\tau_1 e^{-\mu\tau_1} + (1-q)\right]}{b_1 b_2 b_3 b_4 - \eta\delta\gamma b_1 b_2 - (1-\eta)\delta\gamma\epsilon_1\epsilon_2} < 0.$$

$$\frac{\partial \mathcal{R}_0}{\partial \alpha} = -\frac{\beta\epsilon_2 \left[q\epsilon_1 e^{-\mu\tau_1} + (1-q)b_1\right](b_1 b_2 b_3 - \eta\delta\gamma b_1 b_2)}{\left(b_1 b_2 b_3 b_4 - \eta\delta\gamma b_1 b_2 - (1-\eta)\delta\gamma\epsilon_1\epsilon_2\right)^2} < 0.$$

In addition, the delay effect τ_1 also negatively affects the dynamics of disease spread, because the corresponding sensitivity expression shows that τ_1 is inversely proportional to the disease spread behavior.

$$\frac{\partial \mathcal{R}_0}{\partial \tau_1} = -\frac{\beta\epsilon_1\epsilon_2 b_4 q\mu e^{-\mu\tau_1}}{b_1 b_2 b_3 b_4 - \eta\delta\gamma b_1 b_2 - (1-\eta)\delta\gamma\epsilon_1\epsilon_2} < 0.$$

This conclusion suggests that a longer delay period causes a decrease in the value of $\mathcal{R}_0$, which means that the spread of TB in the population is reduced.

The numerical values of the parameters in the proposed delayed TB model are shown in the Figure 2. The graphical representation gives a clear comparison of the epidemiological parameters that are included in the spread behavior of the disease. According to the analysis, the greatest number of the parameters is the recruitment rate Λ. Additionally, the parameters of the transmission, treatment, progression and recovery of the infection have significant effects on the $\mathcal{R}_0$ value. The graph uses a logarithmic scale to represent the different parameters on the same scale and to enhance the graphical presentation. The sensitivity analysis shows how the $\mathcal{R}_0$ $\mathcal{R}_0$ depends on the various parameters of the model as shown in Figure 3. Parameters that have positive sensitivity indices contribute to increase in transmission potential of TB while parameters with negative sensitivity indices contribute to the reduction of the spread of the disease. Numerical results indicate that the transmission parameter β, the progression parameters ϵ_1 and ϵ_2, and the relapse parameter δ all have a positive effect on the transmission parameter $\mathcal{R}_0$. On the other hand, treatment parameter γ, natural death rate μ, recovery parameter α and delay parameter τ_1 have negative sensitivity indices highlighting their importance in controlling disease transmission. Moreover, the graphical depiction of the sensitivity indices offers a direct comparison of the relative effects that each parameter has on the disease dynamics. Therefore, reducing transmission of TB among the population by increasing treatment efficiency and delay effects will be effective.

Figure 4 shows how the $\mathcal{R}_0$ changes as a function of the Contact rate β. From the graphical results it is found that the transmission parameter is a significant factor to increase $\mathcal{R}_0$ as it increases. The behavior is an expression of the positive effect of the transmission rate on the spread of TB in the population. In addition, the curve is rising indicating the need to reduce the contact and transmission rate to control the dynamics of the disease. The Figure 5 shows the effect of the recovery rate α on the $\mathcal{R}_0$. The graphical results show that the larger the recovery parameter, the smaller the value of $\mathcal{R}_0$, which in turn means that the transmission potential of TB

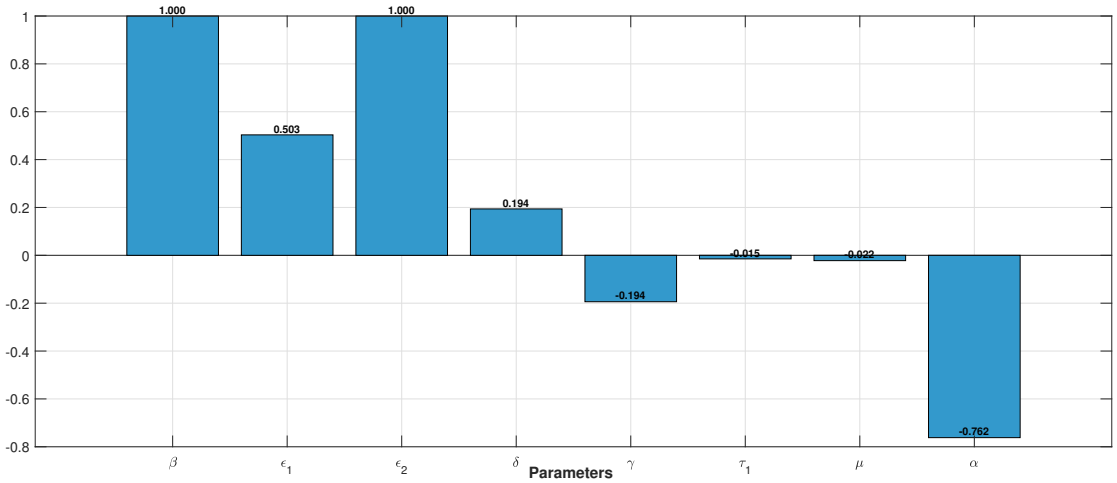

Figure 3: Parameters.

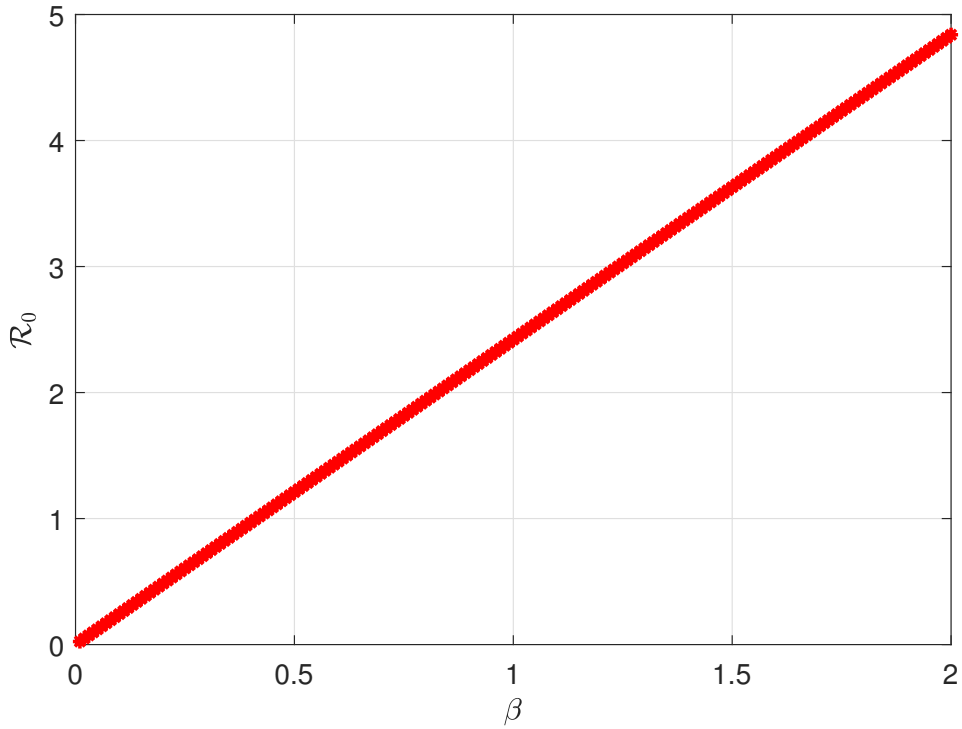

Figure 4: Variation of $\mathcal{R}_0$ with respect to β.

within the population is smaller. This behavior substantiates the adverse effect of the recovery parameter on the dynamics of the disease. Therefore, better recovery rates, achieved by sound treatment methods, can make an important contribution to the control of TB. Figure 6 shows the change of the $\mathcal{R}_0$ as a function of treatment rate γ. The graphical results indicate that the larger the treatment parameter, the smaller the value of $\mathcal{R}_0$, which in turn decreases the transmission potential of the TB disease in the population. This behavior shows that the treatment parameter has a negative effect on the disease dynamics. As a result, a higher treatment rate is an effective way of controlling and reducing the spread of TB. Figure 7 shows how the $\mathcal{R}_0$ changes as the natural mortality rate μ changes. The plots suggest that the larger the value of μ is, the smaller the value of $\mathcal{R}_0$ is, which means that the more the transmission potential of TB in the population is reduced. This behavior verifies the negative impact of the parameter for natural death on the dynamics of the disease. Hence, higher values of μ contribute toward reducing the spread of TB in the community. Figure 8 shows how the $\mathcal{R}_0$ changes as function of the death rate parameter σ_1 due to the disease. The graphical results show that as the value of σ_1 increases, the value of $\mathcal{R}_0$ decreases and the transmission of TB in the population is also reduced. This behaviour is consistent with the adverse effect of the disease-induced death parameter on disease spread. Therefore, the greater the value of σ_1 is, the more

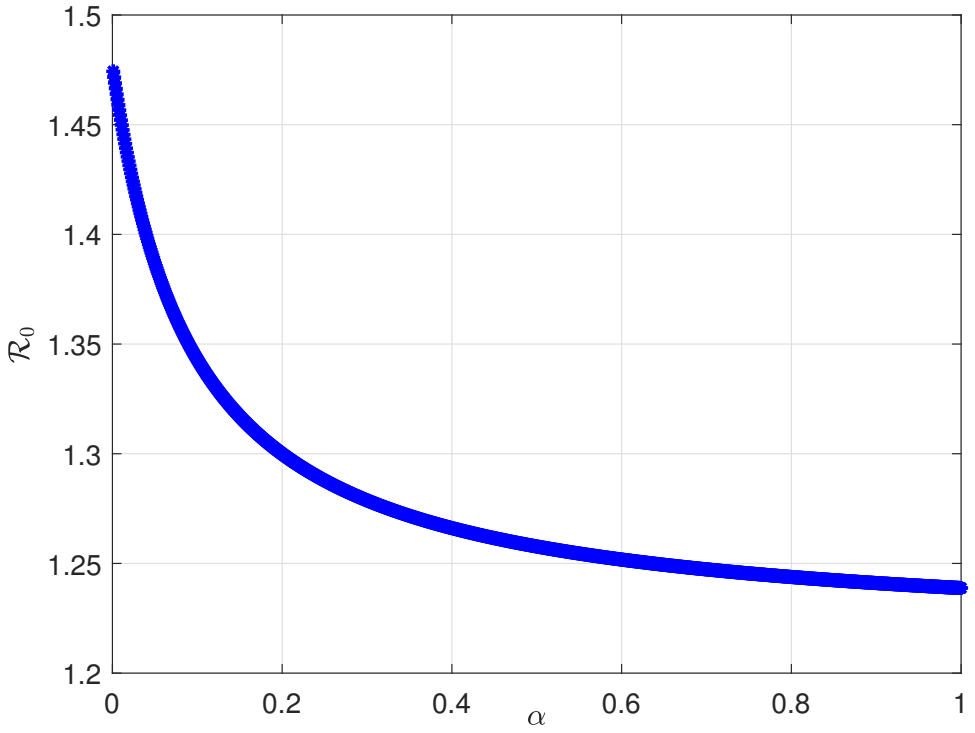

Figure 5: Variation of $\mathcal{R}_0$ with respect to α.

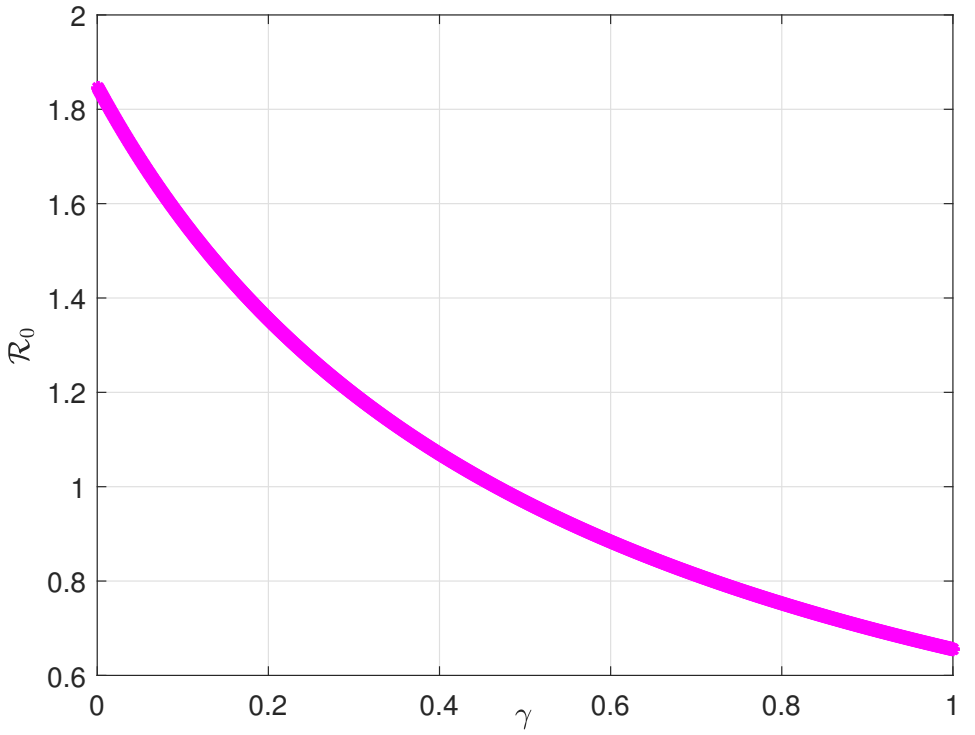

Figure 6: Variation of $\mathcal{R}_0$ with respect to γ.

transmission potential of TB will be reduced. The Figure 9 shows the effect of the ratio of the disease induced death parameter during treatment σ_2 on the $\mathcal{R}_0$. The graphical solutions show that as the value of σ_2 increases the value of $\mathcal{R}_0$ decreases, which lowers the transmission potential of TB in the population. This behavior is in line with the negative effect that the treatment-related disease-induced death parameter had on the disease dynamics. So increasing the value of σ_2 will help reduce the spread of TB. The

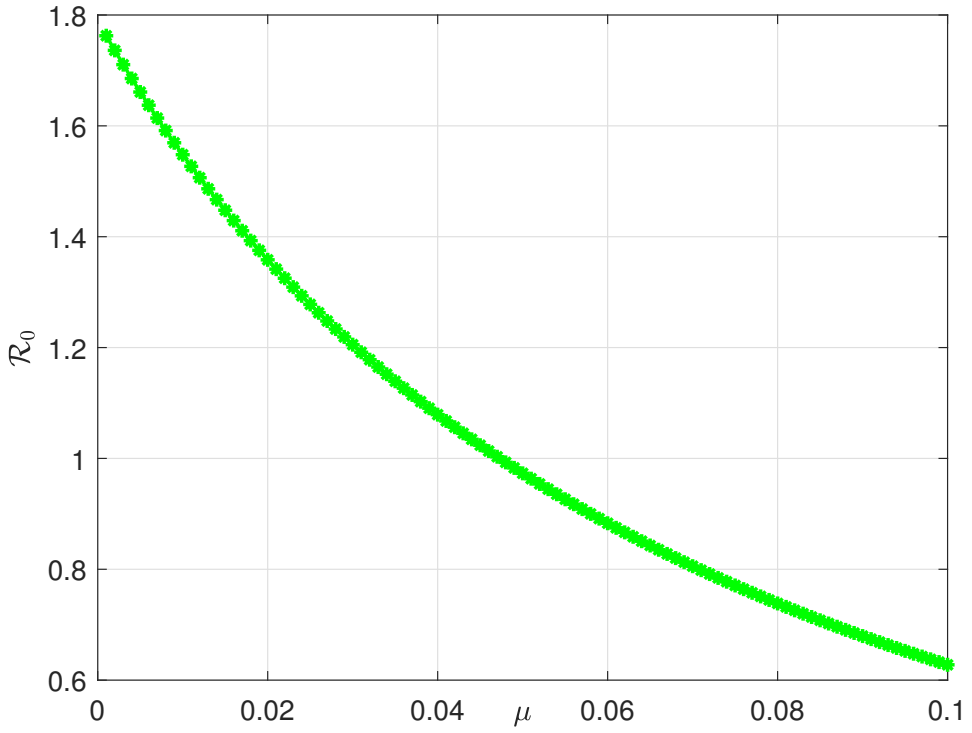

Figure 7: Variation of $\mathcal{R}_0$ with respect to μ.

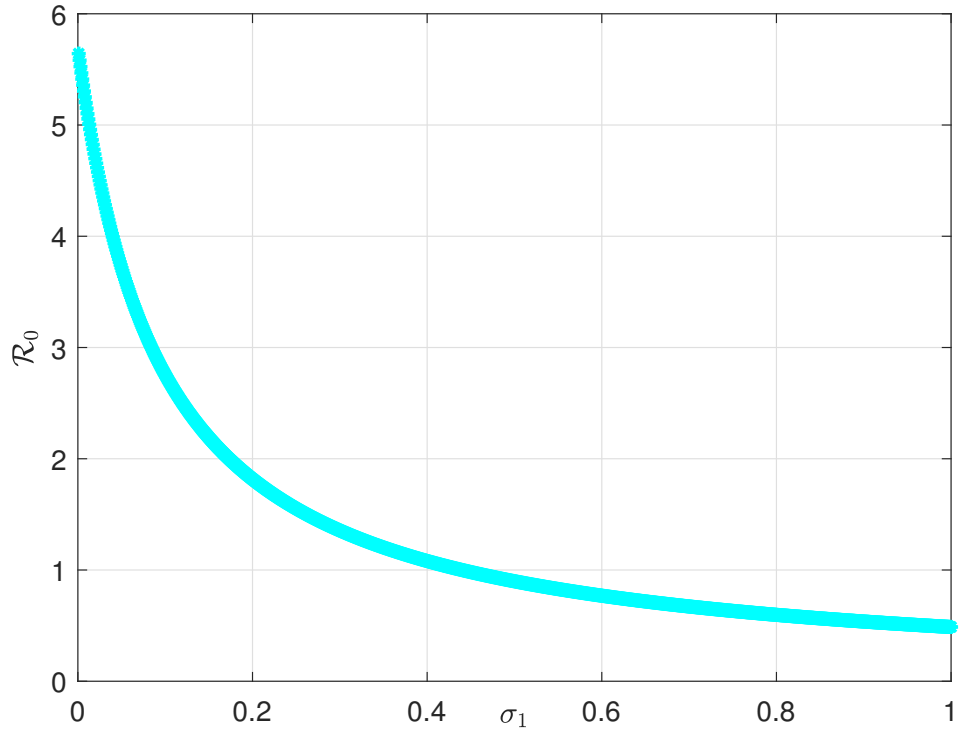

Figure 8: Variation of $\mathcal{R}_0$ with respect to σ_1.

Figure 10 shows the changing of the $\mathcal{R}_0$ as a function of the treatment failure parameter η. As the value of η is increased, the value of $\mathcal{R}_0$ is also increased, according to the graphical results, which shows that the spread behavior of TB within the population becomes better and better as the value of η is increased. This is behavior that verifies that the treatment failure parameter is having a positive effect on the transmission of the disease. Thus, a higher value for η will play an important role in enhancing the transmissibility of

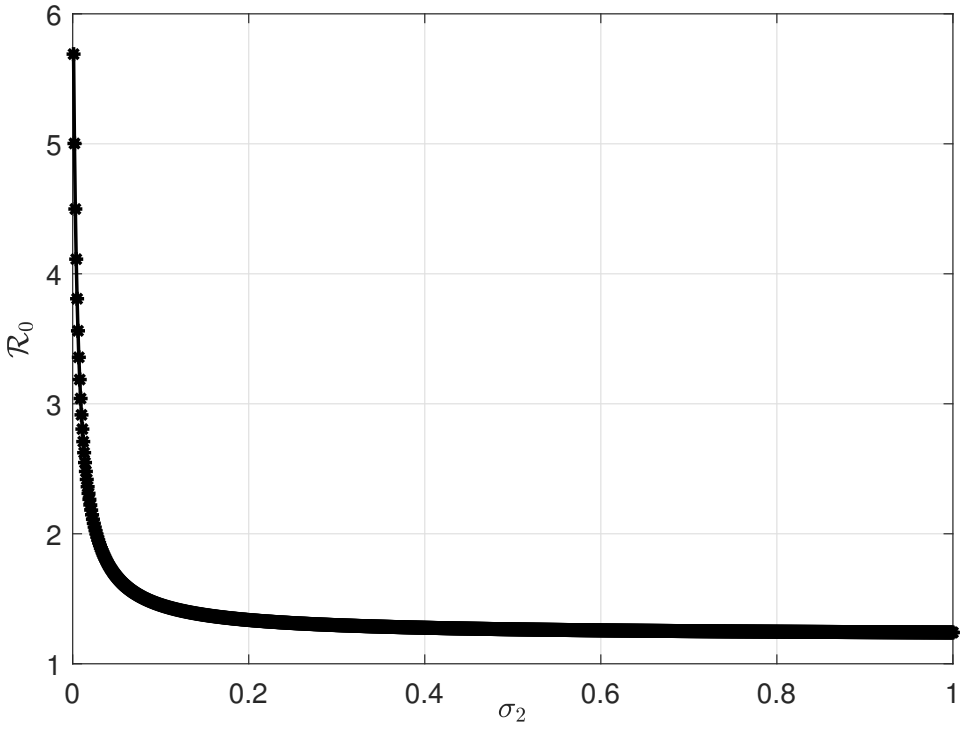

Figure 9: Variation of $\mathcal{R}_0$ with respect to σ_2.

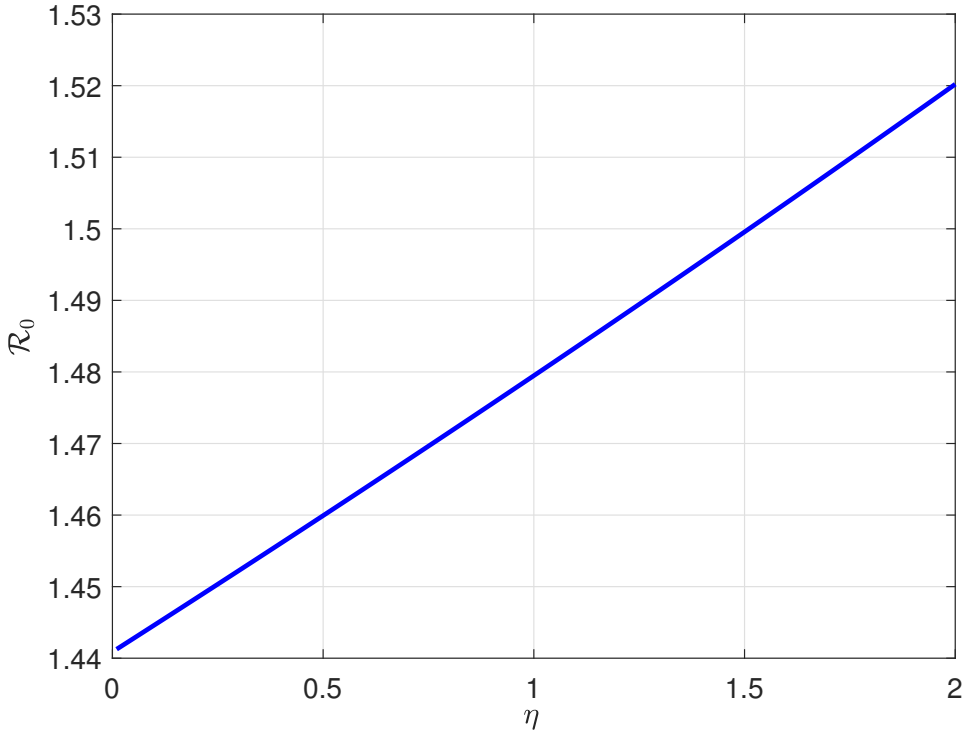

Figure 10: Variation of $\mathcal{R}_0$ with respect to η.

TB. The Figure 11 shows the change of the $\mathcal{R}_0$ as the progression rate parameter ϵ_1 changes. The graphical solutions show that the higher the value of ϵ_1, the higher the value of $\mathcal{R}_0$, which strengthens the transmission potential of TB in the population. This behavior supports the positive effect of the progression parameter on the spread of the disease. Therefore, an increase in the value of ϵ_1 is an important factor in enhancing the transmissibility of TB.

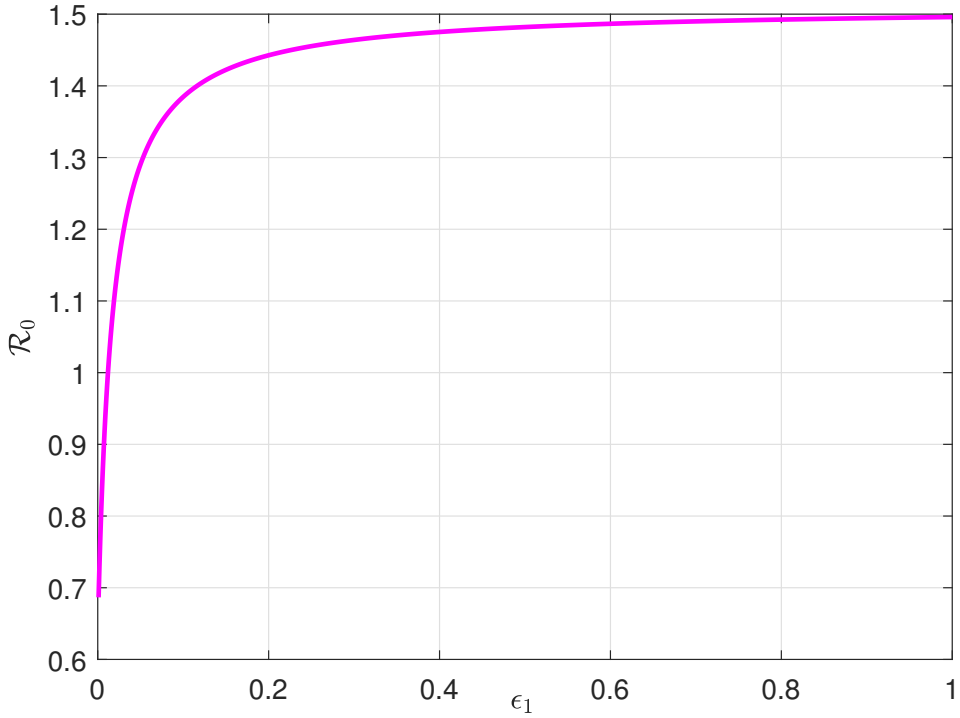

Figure 11: Variation of $\mathcal{R}_0$ with respect to ϵ_1.

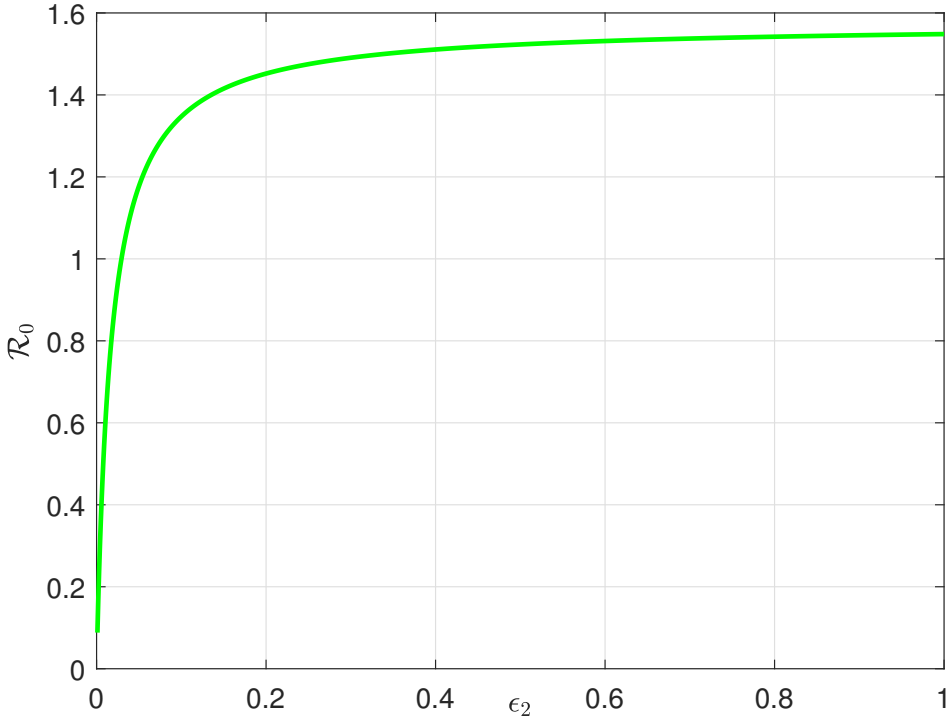

Figure 12: Variation of $\mathcal{R}_0$ with respect to ϵ_2.

The Figure 12 shows the dependence of the $\mathcal{R}_0$ on the progression rate parameter ϵ_2. The graphical solution allows us to see that the larger the value of ϵ_2 the larger the value of $\mathcal{R}_0$ which makes the spread behavior of TB in the population more powerful the larger the value of ϵ_2. This behavior is evidence of the positive effect of the progression parameter on the transmission of the disease. Therefore, any increase in ϵ_2 will make a substantial addition to the transmission potential of TB.

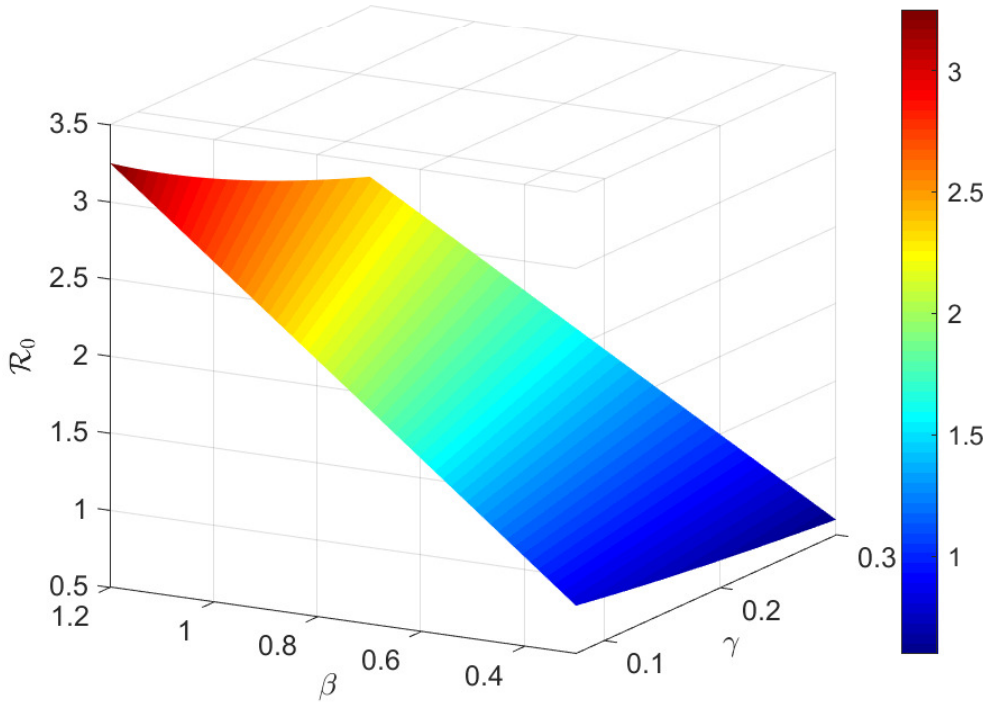

Figure 13: Three-dimensional surface plot of $\mathcal{R}_0$ with respect to β and γ.

The combined effect of the parameters of the transmission parameter β and treatment parameter γ on the $\mathcal{R}_0$ is shown in the Figure 13 below. The graphical solutions show that the higher the rate of transmission the greater the value of $\mathcal{R}_0$ and the lower the rate of transmission the less the dynamics of the disease. The three dimensional surface plot clearly shows that the spread of TB is positively affected by β and negatively affected by γ. Thus, decreasing the transmission rate and increasing the efficiency of treatment is important in keeping the disease under control in the population. Figure 14 shows the combined roles of natural mortality parameter μ and recovery parameter α on the $\mathcal{R}_0$. From the graphical results it is found that as the values of μ and α are increased the value of $\mathcal{R}_0$ is decreased which in turn reduces the spread behavior of TB in the population. The three dimensional surface plot illustrates the negative effect of both parameters on disease transmission. This indicates that a greater rate of recovery and people's natural excretion are crucial in the management of TB. The combined effect of the relapse parameter δ and the treatment failure parameter η on the $\mathcal{R}_0$ is shown in the Figure 15. The graphical outputs show that as the values of both δ and η are raised, the value of $\mathcal{R}_0$ is raised, which means that the spread behavior of TB in the population is improved. The spread of the disease can be clearly observed from the 3-D surface plot which shows that both parameters are positively affecting the disease. This results in a greater potential of transmission of TB via higher relapses and treatment failure rates. Figure 16 shows the effect of the progression rate parameters ϵ_1 and ϵ_2 on the $\mathcal{R}_0$. The graphical outputs suggest that the higher the values of ϵ_1 and ϵ_2 the more close the TB spread behavior in the population, that is, the higher the value of $\mathcal{R}_0$. The three dimensional surface plot clearly shows the positive effect both parameters of progression have on the spread of the disease. The result is that higher rates of progression will also raise the risk of TB being transmitted. The change of the $\mathcal{R}_0$ as a function of the delay parameter τ_1 is shown in Figure 17. The graphical results demonstrate that when the delay parameter is increased, the value of $\mathcal{R}_0$ lowers, indicating a decrease in the population's TB spread behavior. This behaviour is consistent with the downward impact that the delay parameter has on the transmission of the disease. Thus, the longer the delay periods the more they will help to regulate the transmission potential of TB. This Figure 18 shows the dependence of the $\mathcal{R}_0$ on the progression parameter ϵ_1 for different values of the delay parameter τ_1. The graphical results show that as ϵ_1 is increased the value of the transmission parameter $\mathcal{R}_0$ is increased, as the delay parameter is increased the transmission parameter of TB is decreased. In addition, the family of curves illustrates the important role of the delayed effect in the transmission of the disease. Thus, the larger the value of the delay the more it helps to limit the spread of TB in the population. The graphical sensitivity analysis shows how the $\mathcal{R}_0$ of the proposed model for TB is affected by the different epidemiological parameters. The results show that the transmission parameter β, progression parameters ϵ_1 and ϵ_2, relapse parameter δ and treatment failure parameter η are all increasing factors for $\mathcal{R}_0$ which make the transmission potential of TB in the population increase. The recovery parameter α, treatment parameter γ, the natural mortality rate μ and the delay parameter τ_1, however, have negative effects on $\mathcal{R}_0$ and consequently help to reduce the spread of the disease. Moreover, the behaviour of the graph is in line with the theoretically calculated sensitivity analysis. The results of the numerical simulations are clear: An increase in the treatment efficiency and delay effects can be important to decrease the

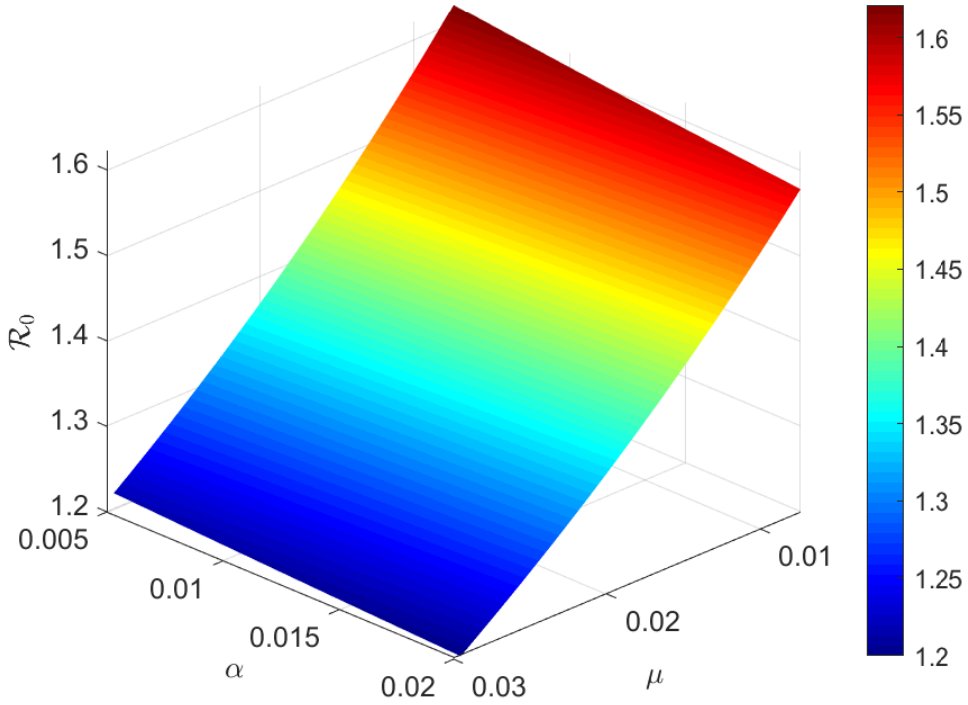

Figure 14: Three-dimensional surface plot of $\mathcal{R}_0$ with respect to μ and α.

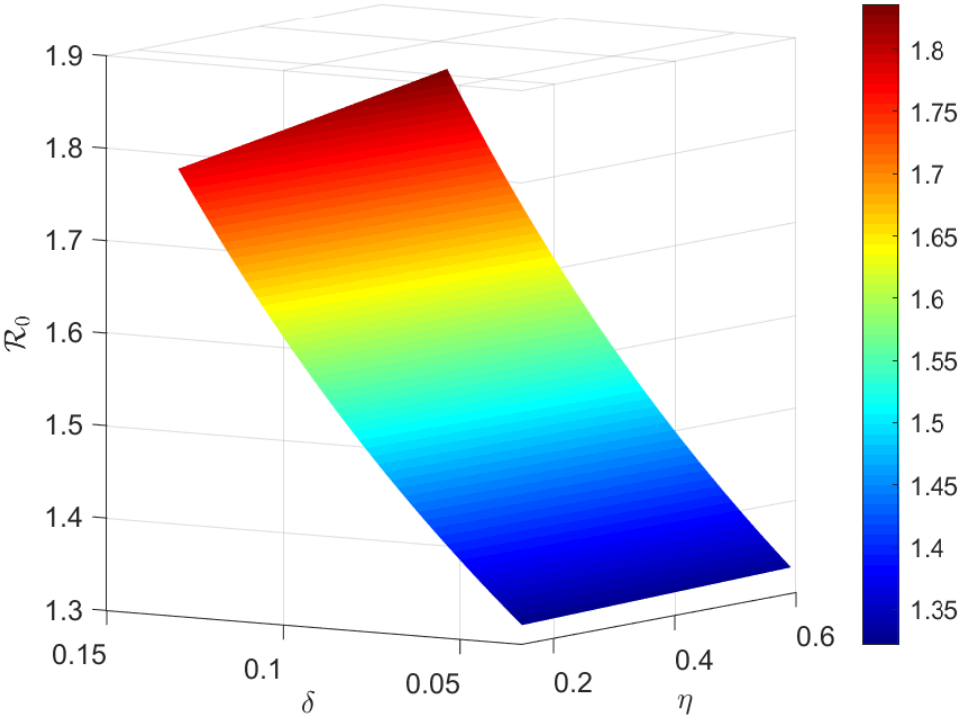

Figure 15: Three-dimensional surface plot of $\mathcal{R}_0$ with respect to δ and η.

transmission of TB while an increase in the transmission and progression rates can be important to increase the persistence of the disease in the population.

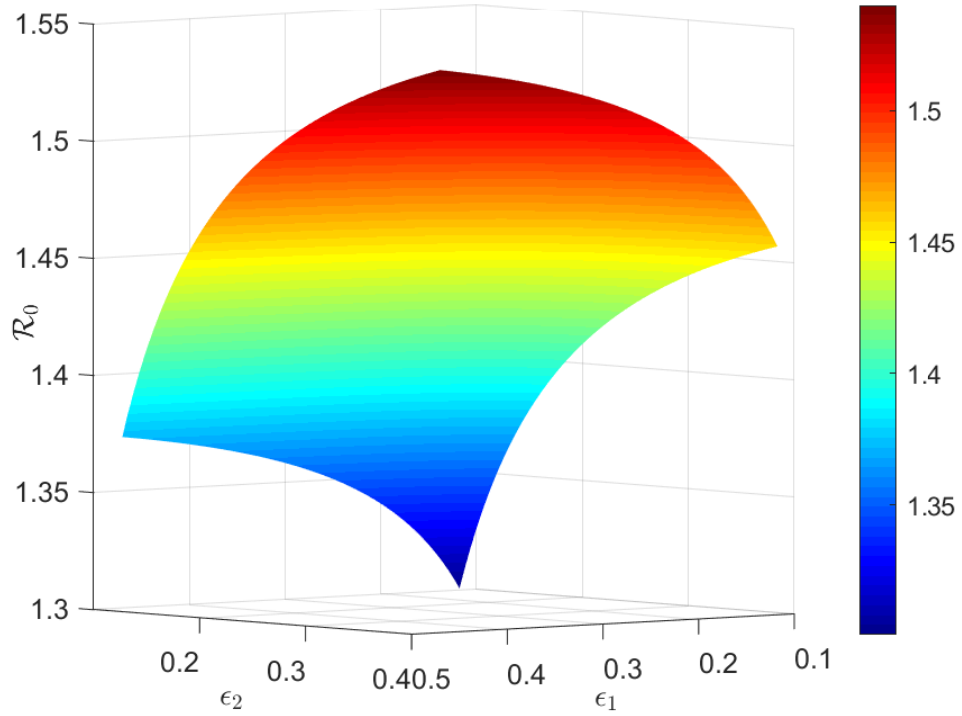

Figure 16: Three-dimensional surface plot of $\mathcal{R}_0$ with respect to ϵ_1 and ϵ_2.

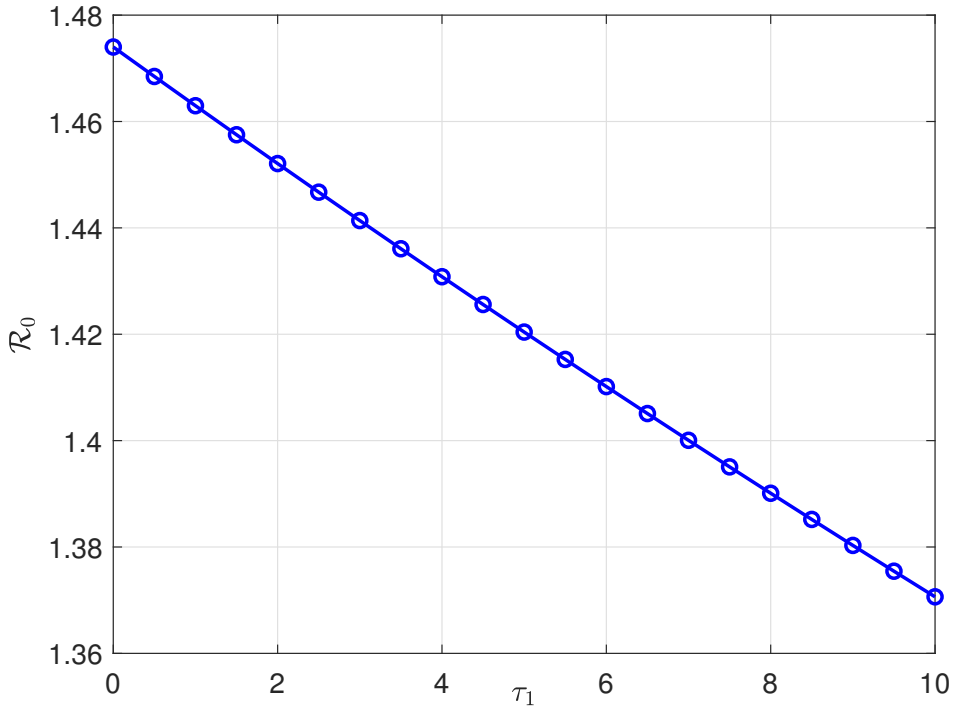

Figure 17: Variation of $\mathcal{R}_0$ with respect to τ_1.

3.1. Biological interpretation of time delay

The delay parameter τ_1 in this proposed TB model can biologically include the time required for diagnosis, treatment initiation, recovery, or the time from latent TB to active infectious TB. The value of $\tau_1 = 2$ represents an approximate two-year delay period which reflects the actual epidemiological scenario in KPK Province Pakistan, where individuals suffering from TB may be

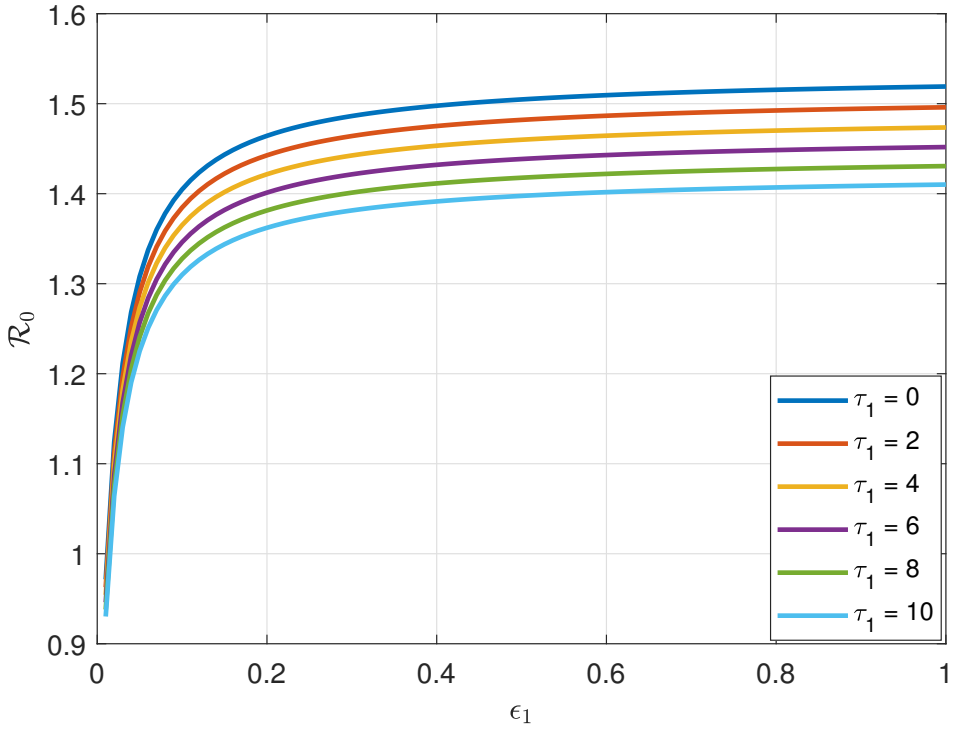

Figure 18: Variation of $\mathcal{R}_0$ with respect to ϵ_1 at different values of τ_1.

in treatment for a lengthy period before being completely diagnosed, treated and recovered. Apart from this, there are also various socioeconomic and healthcare associated factors in KPK which are responsible for this delay, such as lack of healthcare facilities in rural areas, lack of timely laboratory diagnosis, lack of knowledge about the symptoms of TB, non-completion of treatment, poverty, malnutrition, and difficulty accessing healthcare services. This means that the infected person can stay in either latent state or treatment stage for a long period of time before recovering. It is observed from the graphical and analytical results that the spread behavior of TB in the population are reduced by decreasing the value of the $\mathcal{R}_0$ with increasing the value of the delay parameter. Biologically, it means that if treatment is monitored closely, progressed at an appropriate rate and medically managed in a timely fashion, the spread of TB can be greatly slowed and the disease contained in the community.

4. Numerical simulations

The dynamical behavior of the proposed TB model is investigated using the NSFD approach. The continuous model's key qualitative characteristics, such as positivity, boundedness, and solution stability, are preserved by the NSFD scheme. Application of the NSFD technique results in a system of equations which are discretized in a dynamically consistent way, whilst retaining good numerical stability and representing the spread behavior of TB. Hence, the NSFD approach is a good numerical tool for the analysis of the proposed delayed TB model.

4.1. Nonstandard finite difference method

The stability of the SEIR model's NSFD technique at the DFE point will be covered in this section.

$$S^{n+1} = \frac{S^n + h\Lambda}{1 + h\left(\frac{\beta e^{-\mu\tau_1} I^n}{N^n} + \mu\right)}, \tag{17}$$

$$E_1^{n+1} = \frac{E_1^n + hq\frac{\beta e^{-\mu\tau_1} S^n I^n}{N^n} + h(1-\eta)\delta T^n}{1 + hb_1}, \tag{18}$$

$$E_2^{n+1} = \frac{E_2^n + h(1-q)\frac{\beta S^n I^n}{N^n} + h\epsilon_1 E_1^n}{1 + hb_2}, \tag{19}$$

$$I^{n+1} = \frac{I^n + h\epsilon_2 E_2^n + h\eta\delta T^n}{1 + hb_3}, \tag{20}$$

$$T^{n+1} = \frac{T^n + h\gamma I^n}{1 + hb_4}, \tag{21}$$

$$R^{n+1} = \frac{R^n + h\alpha T^n}{1 + h\mu}. \tag{22}$$

4.2. Convergence analysis of the NSFD scheme

The convergence and stability of the proposed NSFD is studied at DFE point in this section. The Jacobian matrix associated with the NSFD scheme is:

$$J(E_0) = \begin{bmatrix} \frac{1}{1+h\mu} & 0 & 0 & -\frac{h\beta e^{-\mu\tau_1}}{1+h\mu} & 0 & 0 \\ 0 & \frac{1}{1+hb_1} & 0 & \frac{hq\beta e^{-\mu\tau_1}}{1+hb_1} & \frac{h(1-\eta)\delta}{1+hb_1} & 0 \\ 0 & \frac{h\epsilon_1}{1+hb_2} & \frac{1}{1+hb_2} & \frac{h(1-q)\beta}{1+hb_2} & 0 & 0 \\ 0 & 0 & \frac{h\epsilon_2}{1+hb_3} & \frac{1}{1+hb_3} & \frac{h\eta\delta}{1+hb_3} & 0 \\ 0 & 0 & 0 & \frac{h\gamma}{1+hb_4} & \frac{1}{1+hb_4} & 0 \\ 0 & 0 & 0 & 0 & \frac{h\alpha}{1+h\mu} & \frac{1}{1+h\mu} \end{bmatrix}.$$

The Jacobian matrix is of a block-type structure and some eigenvalues can be easily obtained from the diagonal blocks. Hence,

$$\lambda_1 = \frac{1}{1 + h\mu}, \qquad \lambda_6 = \frac{1}{1 + h\mu}.$$

The other eigenvalues correspond to the infected subsystem matrix.

$$\begin{bmatrix} \frac{1}{1+hb_1} & 0 & \frac{hq\beta e^{-\mu\tau_1}}{1+hb_1} & \frac{h(1-\eta)\delta}{1+hb_1} \\ \frac{h\epsilon_1}{1+hb_2} & \frac{1}{1+hb_2} & \frac{h(1-q)\beta}{1+hb_2} & 0 \\ 0 & \frac{h\epsilon_2}{1+hb_3} & \frac{1}{1+hb_3} & \frac{h\eta\delta}{1+hb_3} \\ 0 & 0 & \frac{h\gamma}{1+hb_4} & \frac{1}{1+hb_4} \end{bmatrix}.$$

It follows that

$$|\lambda_i| < 1, \qquad i = 1, 2, \ldots, 6.$$

Setting all model parameters and the step size $h > 0$ positive. So, the DFE point of the NSFD scheme is LAS if

$$\mathcal{R}_0 < 1.$$

4.3. Positivity analysis

Theorem 4.1. Assume that the initial conditions

$$S^0, E_1^0, E_2^0, I^0, T^0, R^0$$

are positive. Then, the NSFD scheme is positive for all $n \geq 0$, that is,

$$S^{n+1} > 0, \quad E_1^{n+1} \geq 0, \quad E_2^{n+1} \geq 0, \quad I^{n+1} \geq 0, \quad T^{n+1} \geq 0, \quad R^{n+1} \geq 0.$$

Proof. Discuss the NSFD scheme.

$$S^{n+1} = \frac{S^n + h\Lambda}{1 + h\left(\frac{\beta e^{-\mu\tau_1} I^n}{N^n} + \mu\right)},$$

$$E_1^{n+1} = \frac{E_1^n + hq\frac{\beta e^{-\mu\tau_1} S^n I^n}{N^n} + h(1-\eta)\delta T^n}{1 + hb_1},$$

$$E_2^{n+1} = \frac{E_2^n + h(1-q)\frac{\beta S^n I^n}{N^n} + h\epsilon_1 E_1^n}{1 + hb_2},$$

$$I^{n+1} = \frac{I^n + h\epsilon_2 E_2^n + h\eta\delta T^n}{1 + hb_3},$$

$$T^{n+1} = \frac{T^n + h\gamma I^n}{1 + hb_4},$$
$$R^{n+1} = \frac{R^n + h\alpha T^n}{1 + h\mu}.$$

All parameters and initial conditions are positive, so for all $n \geq 0$ the numerators and denominators of all equations are positive. Hence,

$$S^{n+1} \geq 0, \quad E_1^{n+1} \geq 0, \quad E_2^{n+1} \geq 0, \quad I^{n+1} \geq 0, \quad T^{n+1} \geq 0, \quad R^{n+1} \geq 0.$$

Hence the suggested NSFD scheme maintains the positivity of all state variables. □

4.4. Boundedness of the NSFD scheme

Theorem 4.2. Assume that the starting conditions are non-negative and finite values. Then the solutions of the proposed NSFD scheme are bounded for all $n \geq 0$.

Proof. Let

$$N^n = S^n + E_1^n + E_2^n + I^n + T^n + R^n.$$

If we add all equations of the NSFD scheme, we get

$$N^{n+1} \leq N^n + h\Lambda - h\mu N^n.$$

Thus,

$$N^{n+1} \leq \frac{N^n + h\Lambda}{1 + h\mu}.$$

By repetition, it follows that

$$N^n \leq \frac{\Lambda}{\mu}, \qquad \forall n \geq 0.$$

Therefore, the NSFD scheme has uniformly bounded all its state variables in the feasible region.

$$\Omega = \left\{ (S, E_1, E_2, I, T, R) \in \mathbb{R}_+^6 : N^n \leq \frac{\Lambda}{\mu} \right\}.$$

Hence, the proposed NSFD scheme is bounded. □

4.5. Consistency analysis

Taylor series expansion is used to test the consistency of the proposed NSFD scheme. For the susceptible population consider the following equation:

$$S^{n+1} = \frac{S^n + h\Lambda}{1 + h\left(\frac{\beta e^{-\mu\tau_1} I^n}{N^n} + \mu\right)}.$$

Using the Taylor's series for expansion of S^{n+1} yields

$$S^{n+1} = S^n + h\frac{dS}{dt} + O(h^2).$$

The substitution into the NSFD equation and simplification yields

$$\frac{dS}{dt} = \Lambda - \frac{\beta e^{-\mu\tau_1} S I}{N} - \mu S,$$

which agrees with the original continuous model, in the same way, the following equations yield the following:

$$\frac{dE_1}{dt} = q\frac{\beta e^{-\mu\tau_1} S I}{N} - b_1 E_1 + (1 - \eta)\delta T,$$
$$\frac{dE_2}{dt} = (1 - q)\frac{\beta S I}{N} + \epsilon_1 E_1 - b_2 E_2,$$
$$\frac{dI}{dt} = \epsilon_2 E_2 + \eta\delta T - b_3 I,$$
$$\frac{dT}{dt} = \gamma I - b_4 T,$$

and

$$\frac{dR}{dt} = \alpha T - \mu R.$$

Thus, the proposed NSFD scheme is in line with the original SEITR TB model.

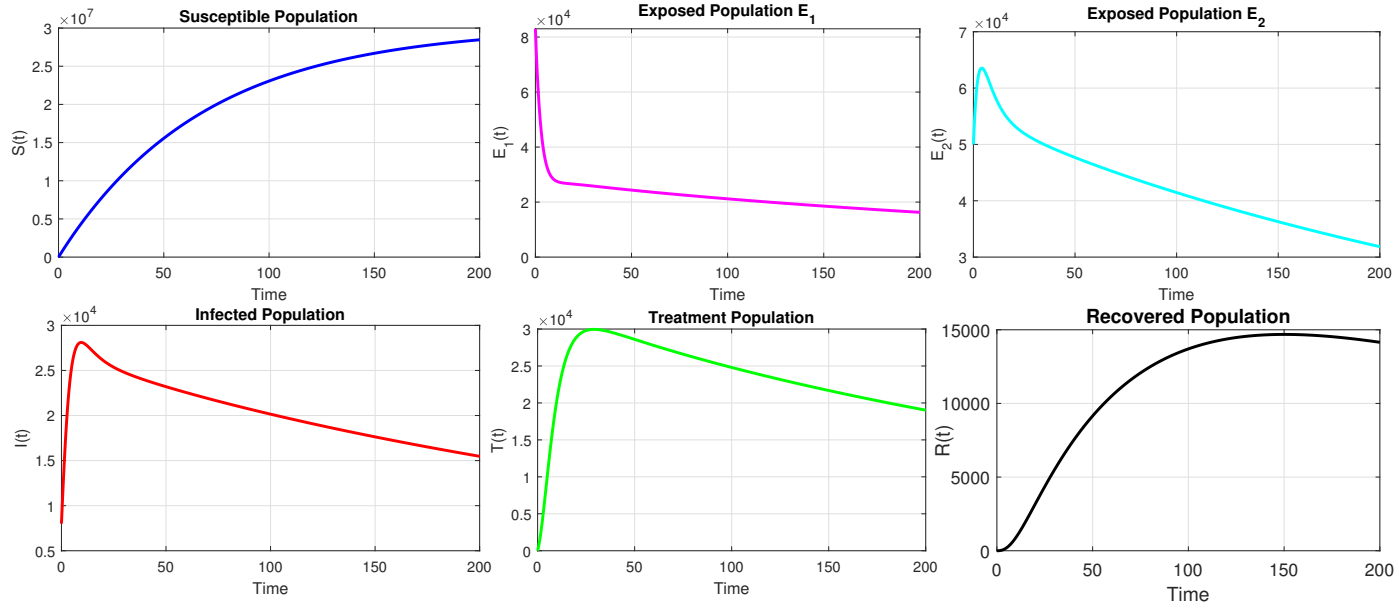

Figure 19: Simulation results of NSFD scheme at the DFE.

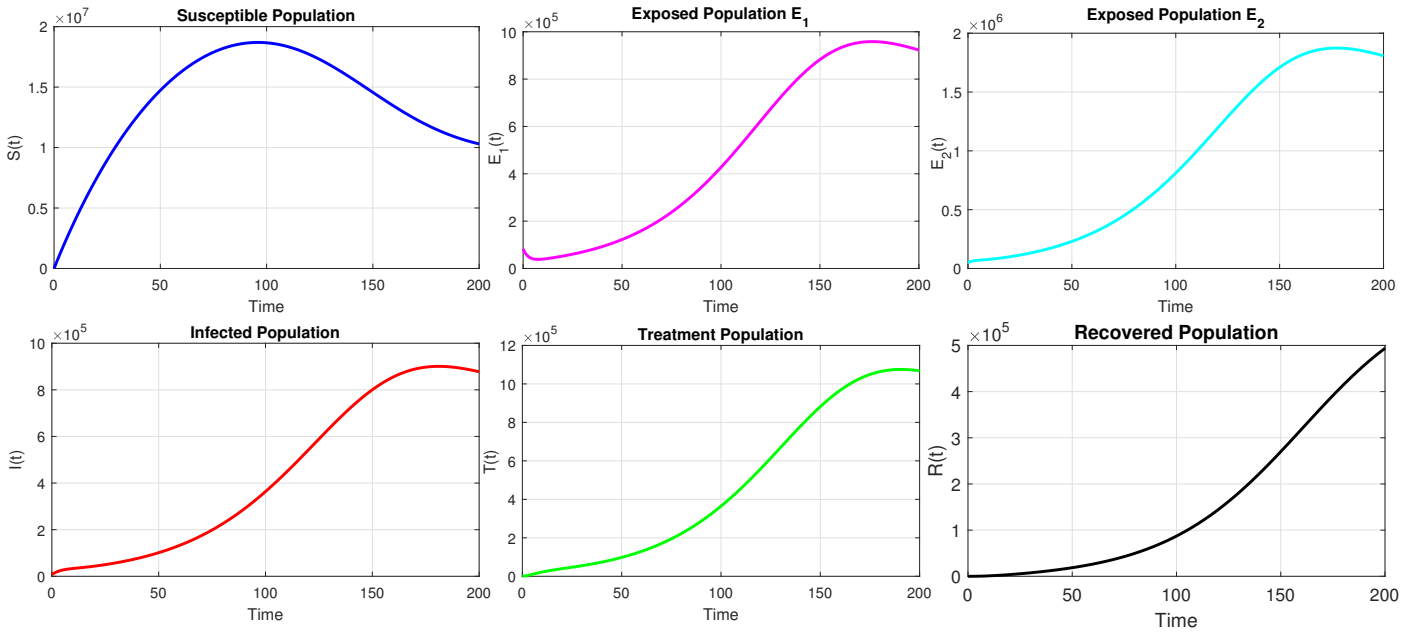

Figure 20: Simulation results of NSFD scheme at the EE.

4.6. Numerical analysis

The numerical simulations of the proposed delayed TB model using the NSFD scheme show the time evolution of each compartment of the epidemiology separately. The graphical results show that both exposed classes E_1 and E_2 as well as infected population I tend to decrease slowly with time demonstrating elimination of infections from the population. Moreover, the numbers of the susceptible, treatment, and recovered populations approach stable equilibrium values, thereby verifying the dynamical consistency and stability of the NSFD numerical scheme. The results of this analysis show that the system is converging to the DFE state for $\mathcal{R}_0 < 1$ which is consistent with the analytical conclusion. In this Figure 19 the step size is $h = 0.5$. The numerical simulations on the proposed delayed TB model via the NSFD scheme show the temporal evolutions of the individual compartments of the epidemiological model, respectively. From the graphical results in Figure 20, it is seen that the susceptible population grows initially and then stabilizes over time. Additionally, the exposed classes E_1 and E_2 and the infected population I reduce slowly over time, further demonstrating that disease is being diminished in the population. The treatment and recovered compartments also converge

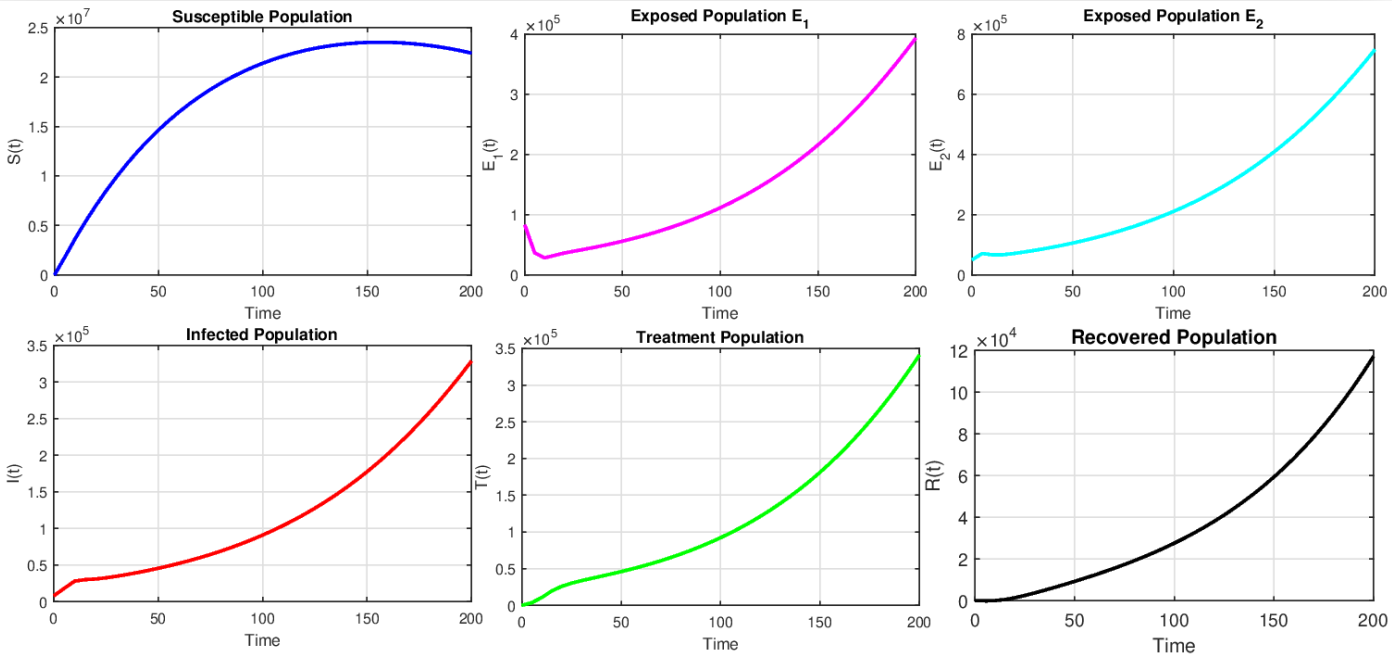

Figure 21: Simulation results of NSFD scheme at large step size $h = 5$.

towards stable levels, showing the effectiveness and stability of the numerical scheme NSFD. Furthermore, the simulations show that if $\mathcal{R}_0 > 1$, the disease stays within the population and the system evolves towards the EE state. Over time the exposed compartments reach positive values while the infected ones reach their equilibrium, which indicates persistence of TB in the community. Further simulation tests were carried out with a greater time step size (h=5) compared with the smaller time step size used in previous tests (h=0.5) to further investigate the numerical robustness of the proposed NSFD scheme. All state variables are positive, bounded and tend to the equilibrium values without any numerical oscillations or divergence as shown in Figure21. The results show that the behaviour of the discrete model obtained with the proposed NSFD scheme has the same qualitative characteristics as the continuous model even for the relatively large time step used in the present study. This number behavior is in line with the dynamically consistent construction of the NSFD method, and further validates the robustness and reliability of the NSFD method in solving delayed epidemiology models.

5. Modified TB model (case II)

Figure 22 shows the modified model structure with the delay in the fast exposed class.

$$\frac{dS}{dt} = \Lambda - \frac{\beta e^{-\mu\tau_1} S(t-\tau) I(t-\tau)}{N} - \mu S(t),$$

$$\frac{dE_1}{dt} = q\frac{\beta e^{-\mu\tau_1} S(t-\tau) I(t-\tau)}{N} - b_1 E_1(t) + (1-\eta)\delta T(t),$$

$$\frac{dE_2}{dt} = (1-q)\frac{\beta e^{-\mu\tau_2} S(t-\tau) I(t-\tau)}{N} + \epsilon_1 E_1(t) - b_2 E_2(t),$$

$$\frac{dI}{dt} = \epsilon_2 E_2(t) + \eta\delta T(t) - b_3 I(t),$$

$$\frac{dT}{dt} = \gamma I(t) - b_4 T(t),$$

$$\frac{dR}{dt} = \alpha T(t) - \mu R(t).$$

where

$$N = S + E_1 + E_2 + I + T + R,$$

and

$$b_1 = \epsilon_1 + \mu, \qquad b_2 = \epsilon_2 + \mu, \qquad b_3 = \gamma + \mu + \sigma_1, \qquad b_4 = \alpha + \mu + \sigma_2.$$

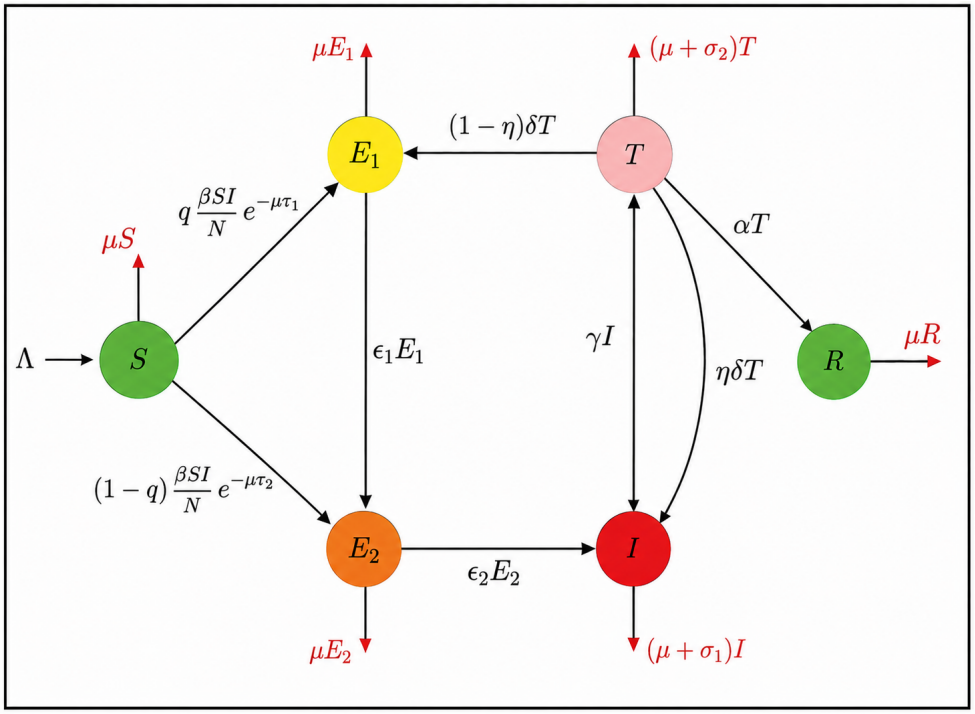

Figure 22: Delay in fast exposed.

5.1. *Updated DFE points, EE points and $\mathcal{R}_{00}$*

5.2. *DFE point*

The DFE point of the proposed delayed SEITR TB model is

$$E_{00} = \left(\frac{\Lambda}{\mu}, 0, 0, 0, 0, 0\right). \tag{23}$$

5.3. $\mathcal{R}_{00}$

The $\mathcal{R}_{00}$ of the model is given by

$$\mathcal{R}_{00} = \frac{\beta\epsilon_2 b_4\left[q\epsilon_1 e^{-\mu\tau_1} + (1-q)b_1 e^{-\mu\tau_2}\right]}{b_1 b_2 b_3 b_4 - \eta\delta\gamma b_1 b_2 - (1-\eta)\delta\gamma\epsilon_1\epsilon_2}. \tag{24}$$

5.4. *EE point*

The EE point of the proposed model is

$$E^{**} = (S^{**}, E_1^{**}, E_2^{**}, I^{**}, T^{**}, R^{**}),$$

where

$$\left(\frac{\Lambda N^{**}}{\mu N^{**} + \beta e^{-\mu\tau_1} I^{**}}, \frac{q\beta e^{-\mu\tau_1} S^{**} I^{**} + (1-\eta)\delta T^{**} N^{**}}{b_1 N^{**}}, \frac{(1-q)\beta e^{-\mu\tau_2} S^{**} I^{**} + \epsilon_1 E_1^{**} N^{**}}{b_2 N^{**}}, \frac{\epsilon_2 E_2^{**} + \eta\delta T^{**}}{b_3}, \frac{\gamma I^{**}}{b_4}, \frac{\alpha T^{**}}{\mu}\right). \tag{25}$$

5.5. *Sensitivity analysis of the modified $\mathcal{R}_{00}$*

Positive effect on $\mathcal{R}_{00}$:

$$\frac{\partial\mathcal{R}_{00}}{\partial\beta} = \frac{\epsilon_2 b_4\left[q\epsilon_1 e^{-\mu\tau_1} + (1-q)b_1 e^{-\mu\tau_2}\right]}{b_1 b_2 b_3 b_4 - \eta\delta\gamma b_1 b_2 - (1-\eta)\delta\gamma\epsilon_1\epsilon_2} > 0.$$

$$\frac{\partial\mathcal{R}_{00}}{\partial\epsilon_1} = \frac{\beta\epsilon_2 b_4 q e^{-\mu\tau_1}}{b_1 b_2 b_3 b_4 - \eta\delta\gamma b_1 b_2 - (1-\eta)\delta\gamma\epsilon_1\epsilon_2} > 0.$$

$$\frac{\partial\mathcal{R}_{00}}{\partial\epsilon_2} = \frac{\beta b_4\left[q\epsilon_1 e^{-\mu\tau_1} + (1-q)b_1 e^{-\mu\tau_2}\right]}{b_1 b_2 b_3 b_4 - \eta\delta\gamma b_1 b_2 - (1-\eta)\delta\gamma\epsilon_1\epsilon_2} > 0.$$

$$\frac{\partial \mathcal{R}_{00}}{\partial \delta} = \frac{\beta\epsilon_2 b_4 \left[q\epsilon_1 e^{-\mu\tau_1} + (1-q)b_1 e^{-\mu\tau_2}\right]\gamma\left(\eta b_1 b_2 + (1-\eta)\epsilon_1\epsilon_2\right)}{\left(b_1 b_2 b_3 b_4 - \eta\delta\gamma b_1 b_2 - (1-\eta)\delta\gamma\epsilon_1\epsilon_2\right)^2} > 0.$$

Negative effect on $\mathcal{R}_{00}$:

$$\frac{\partial \mathcal{R}_{00}}{\partial \gamma} = -\frac{\beta\epsilon_2 b_4 \left[q\epsilon_1 e^{-\mu\tau_1} + (1-q)b_1 e^{-\mu\tau_2}\right]\delta\left(\eta b_1 b_2 + (1-\eta)\epsilon_1\epsilon_2\right)}{\left(b_1 b_2 b_3 b_4 - \eta\delta\gamma b_1 b_2 - (1-\eta)\delta\gamma\epsilon_1\epsilon_2\right)^2} < 0.$$

$$\frac{\partial \mathcal{R}_{00}}{\partial \tau_1} = -\frac{\beta\epsilon_1\epsilon_2 b_4 q\mu e^{-\mu\tau_1}}{b_1 b_2 b_3 b_4 - \eta\delta\gamma b_1 b_2 - (1-\eta)\delta\gamma\epsilon_1\epsilon_2} < 0.$$

$$\frac{\partial \mathcal{R}_{00}}{\partial \tau_2} = -\frac{\beta\epsilon_2 b_1 b_4 (1-q)\mu e^{-\mu\tau_2}}{b_1 b_2 b_3 b_4 - \eta\delta\gamma b_1 b_2 - (1-\eta)\delta\gamma\epsilon_1\epsilon_2} < 0.$$

$$\frac{\partial \mathcal{R}_{00}}{\partial \mu} = -\frac{\beta\epsilon_2 b_4 \left[q\epsilon_1\tau_1 e^{-\mu\tau_1} + (1-q)b_1\tau_2 e^{-\mu\tau_2}\right]}{b_1 b_2 b_3 b_4 - \eta\delta\gamma b_1 b_2 - (1-\eta)\delta\gamma\epsilon_1\epsilon_2} < 0.$$

$$\frac{\partial \mathcal{R}_{00}}{\partial \alpha} = -\frac{\beta\epsilon_2 \left[q\epsilon_1 e^{-\mu\tau_1} + (1-q)b_1 e^{-\mu\tau_2}\right]\left(b_1 b_2 b_3 - \eta\delta\gamma b_1 b_2\right)}{\left(b_1 b_2 b_3 b_4 - \eta\delta\gamma b_1 b_2 - (1-\eta)\delta\gamma\epsilon_1\epsilon_2\right)^2} < 0.$$

The sensitivity analysis of the $\mathcal{R}_{00}$ gives important clues about the role of the parameters of the model on the transmission of TB. Parameters with positive sensitivity indices would tend to make the value of $\mathcal{R}_{00}$ greater and hence make the disease more infectious in the population. On the other hand parameters with negative sensitivity indices decrease the value of $\mathcal{R}_{00}$ and thus help in the control of disease transmission. From the results, it is observed that the transmission rate β, progression rates ϵ_1 and ϵ_2 and the relapse parameter δ have positive impact on the disease dynamics. The recovery and treatment-related parameters, γ and α, on the other hand, have negative effects on the recovery-related $\mathcal{R}_{00}$, along with the two delay parameters, τ_1 and τ_2. This means that the greater the delay and treatment rates, the more that it can be reduced in the community.

5.6. Biological interpretation of time delay

The values of the two time delays, $\tau_1 = 1.3$ years and $\tau_2 = 0.72$ years, are used in the delayed TB model with two time delays. These delays are in months about equal to

$$\tau_1 \approx 15.6 \text{ months}, \qquad \tau_2 \approx 8.64 \text{ months}.$$

The numerical results show that the EE point exists whenever the $\mathcal{R}_{00}$ is.

$$\mathcal{R}_{00} = 1.4521 > 1,$$

which means that TB has been maintained in the population. On the other hand, the DFE is obtained when

$$\mathcal{R}_{00} = 0.9681 < 1,$$

means the disease slowly eradicates from the community. In addition, the results that were obtained demonstrate that the presence of treatment monitoring and supervised medication delay τ_2 with only 0.72 years (≈ 8.64 months) is enough to meaningfully decrease the spread behavior of TB and to achieve the desired epidemiological behavior, even though the latent progression delay τ_1 was reduced from 2 years to 1.3 years. This means that the delay of the treatment causes a greater control over the disease spread than the delay of the latent progression. The first delay parameter τ_1 can be interpreted as the latent incubation period, delayed diagnosis or delayed activation of TB infection, in a biological sense. The second delay parameter τ_2, on the other hand, can refer to a period of supervised treatment, medication adherence, patient isolation, treatment monitoring, post-treatment care, or controlled treatment response post-diagnosis. Within the framework of KPK Province in Pakistan, this delay associated with treatment could be linked to better TB control programs, supervised medication schedules, regular patient follow up, timely initiation of treatment and ongoing surveillance by health authorities. The impact of these preventative measures is to decrease effective contact between infectious and susceptible individuals in a relatively short time, which is why even a moderate delay in the treatment of about 8.64 months can significantly decrease the disease transmission rate. Therefore the treatment monitoring delay parameter is very influential in controlling the dynamics of TB, the reduction of its effective $\mathcal{R}_{00}$ and the stabilization of the epidemiological behavior of the disease within the population.

6. Discussion and conclusion

A nonlinear delayed mathematical model of TB spread behavior has been proposed and analyzed in this study with special focus on epidemiological situation in KPK, Pakistan. Delayed diagnosis, poverty, treatment drop-off, poor access to healthcare and poor monitoring are factors that make TB one of the most deadly infectious diseases in the region. To explore the practical implications of these, the proposed model also includes biologically meaningful time lags for latent disease activity and supervised monitoring of treatment. The basic mathematical features of the model, such as positivity, boundedness, equilibrium points, and the stability behavior were carefully studied. To directly understand the threshold behavior of the disease, the $\mathcal{R}_0$ was derived. The analytic results showed that the DFE is stable when $\mathcal{R}_0 < 1$ and it is unstable when $\mathcal{R}_0 > 1$, and that the EE exists and is stable when $\mathcal{R}_0 > 1$ and unstable when $\mathcal{R}_0 < 1$. Results of the numerical simulations with the use of NSFD scheme strongly corroborated the theoretical results and revealed stable and dynamically consistent solutions. Sensitivity analysis identified the parameters affecting TB transmission to be positively associated when they are transmission- related parameters while the recovery-related and delay-associated parameters significantly lowered TB transmission. The results that are obtained show that there can be significant decreases in the effective reproduction number even with moderate improvements in treatment efficiency and disease monitoring.

This work makes a significant contribution in the inclusion and comparison of two biologically meaningful delay parameters. The first delay time τ_1 corresponds to the latent period of TB infection or the time delay for activation. The model originally used a larger latent delay, about 2 years. However, on introducing the second delay parameter, the value of the first delay parameter was taken as approximately 1.3 years ($\approx$ 15.6 months) while the second delay parameter τ_2 was taken as approximately 0.72 year ($\approx$ 8.64 months). Biologically, the second delay is equivalent to the follow-up of diagnosis, recovery observation, controlled medical supervision, supervised treatment monitoring based on medication adherence, isolation and treatment. The numerical results clearly illustrated that even a small delay of around 8.64 months due to treatment caused a substantial decrease in the dynamics of the disease transmission and consequently the spread of the TB was effectively controlled. This indicates that treatment supervision and ongoing observation of the patient have a greater impact on controlling TB transmission than the extended latent progression delays themselves. The significance of these findings in the context of KPK is noteworthy as many TB patients suffer from irregular treatment schedules, delayed follow-up, poor treatment adherence, and limited healthcare supervision. Improved treatment monitoring systems, availability of TB drugs at all times, better patient follow-up, and intervention strategies based on can significantly decrease the transmission potential of TB in the population. In addition, the NSFD numerical method was very successful in maintaining the positivity, boundedness and dynamicity of the solutions for all the time steps considered. The NSFD scheme presented numerical stability and reliability without causing numerical oscillations, unlike traditional numerical methods, thus showing the ability of the NSFD to solve a nonlinear epidemiological system with delay. The NSFD method, however, maintains all the qualitative characteristics of the continuous system such as positivity, boundedness, and stability, which leads to numerically obtained solution being dynamically consistent and reliable. This feature makes the NSFD scheme an appropriate numerical tool to analyze delayed epidemiological models and facilitates its application to the study of the long-term transmission dynamics of TB. Overall the suggested delayed model of TB is useful both theoretically as well as practically in understanding the spread behavior of TB in KPK, Pakistan. The analytical investigations, sensitivity analysis, biological interpretation and stable numerical simulations can help healthcare authorities and policymakers in developing better intervention and disease control strategies. Taken together, the proposed model for TB transmission and its delayed treatment outcomes is a sound mathematical model to investigate the nature of TB transmission and shows that biological delayed treatment monitoring is an effective mechanism to reduce the spread of the TB epidemic. The results of these findings will provide important inputs for designing evidence-based strategies for TB control in KPK, Pakistan. Extensions of this research could include other biological delays, optimal control schemes, stochastic effects, fractional order dynamics, and spatial diffusion to better capture the complex nature of TB transmission and include such effects in the future.

Data availability

All data are available within the article.

Declaration of competing interest

The authors declare that they have no known competing financial interests or personal relationships that could have appeared to influence the work reported in this manuscript.

Acknowledgment

The author expresses gratitude to the Universiti Sains Malaysia (USM) for their financial support of this paper. Also, we would like to thank the school of mathematical sciences for providing the necessary computing facilities.

Funding

The authors received no specific funding from any public, commercial, or not-for-profit organisation for this research.

References

[1] M. A. Khan, M. Ahmad, S. Ullah, M. Farooq & T. Gul, "Modeling the transmission dynamics of tuberculosis in Khyber Pakhtunkhwa Pakistan", Advances in Mechanical Engineering **11** (2019) 168781401985483. https://doi.org/10.1177/1687814019854835.
[2] World Health Organization, Global tuberculosis report, 2019. https://www.who.int/publications/i/item/global-tuberculosis-report-2019.
[3] M. S. Said, R. Fatima, R. Ahmad, M. B. A. Al Rawi, F. Jan, S. Faisal, I. Khan & A. H. Khan, "Evaluation of social and clinical factors associated with adverse drug reactions among children with drug-resistant tuberculosis in Pakistan", Tropical Medicine and Infectious Disease **10** (2025) 176. https://doi.org/10.3390/tropicalmed10070176.
[4] World Health Organization, Tuberculosis country profiles, 2018. Available online: https://www.who.int/tb/country/data/profiles/en/.
[5] S. Ullah, H. Daud, S. Dass, H. Fanaee-T, H. Kausarian & Alamgir, "Space-time clustering characteristics of tuberculosis in khyber pakhtunkhwa province, pakistan, 2015-2019", International Journal of Environmental Research and Public Health **17** (2020) 1413. https://doi.org/10.3390/ijerph17041413.
[6] World Health Organization, "WHO country cooperation strategy at a glance: Pakistan", World Health Organization, 2018. https://www.who.int/publications/i/item/WHO-CCU-18.02-Pakistan.
[7] S. Falahuddin, L. Khan, M. Iqbal & N. Salahuddin, "Statistical analysis of various risk factors of tuberculosis in district Mardan, Pakistan", Journal of Biostatistics and Epidemiology **2** (2016) 47. https://scispace.com/pdf/statistical-analysis-of-various-risk-factors-of-tuberculosis-451sbtmxwp.pdf
[8] I. Khattak, M. H. Mushtaq, M. U. D. Ahmad, M. S. Khan & J. Haider, "Zoonotic tuberculosis in occupationally exposed groups in Pakistan", Occupational Medicine **66** (2016) 371. https://doi.org/10.1093/occmed/kqw039.
[9] H. Ahmad, I. Inamullah, I. Ali, T. Ahmad, M. Tufail, K. Ahmad & B. N. Murtaza, "Prevalence of brucellosis in human population of district Swat, Pakistan", Pakistan Journal of Zoology **49** (2017) 391. https://doi.org/10.17582/journal.pjz/2017.49.1.sc11.
[10] S. Ullah, H. Daud, S. C. Dass, H. Fanaee-T & A. Khalil, "An eigenspace approach for detecting multiple space-time disease clusters: application to measles hotspots detection in Khyber-Pakhtunkhwa, pakistan", PLOS ONE **13** (2018) e0199176. https://doi.org/10.1371/journal.pone.0199176.
[11] M. Kulldorff & U. Hjalmars, "The knox method and other tests for space-time interaction", Biometrics **55** (1999) 544. https://doi.org/10.1111/j.0006-341x.1999.00544.x.
[12] N. Mantel, "The detection of disease clustering and a generalized regression approach", Cancer research **27** (1967) 209. https://aacrjournals.org/cancerres/article/27/2_Part_1/209/476508/The-Detection-of-Disease-Clustering-and-a.
[13] M. Kulldorff, W. F. Athas, E. J. Feurer, B. A. Miller & C. R. Key, "Evaluating cluster alarms: a space-time scan statistic and brain cancer in Los Alamos, New Mexico", American Journal of Public Health **88** (1998) 1377. https://doi.org/10.2105/ajph.88.9.1377.
[14] D. Birant & A. Kut, "ST-DBSCAN: an algorithm for clustering spatial-temporal data", Data & Knowledge Engineering **60** (2007) 208. https://doi.org/10.1016/j.datak.2006.01.013.
[15] S. Zeb, S. A. Mohd Yatim, S. Lal, A. Kamran, A. Ahmad & M. Rafiq, "Numerical analysis of the NSP epidemic model for campus drinking dynamics", Semarak International Journal of Fundamental and Applied Mathematics **4** (2024) 48. https://doi.org/10.37934/sijfam.4.1.4860.
[16] S. Zeb, M. Bilal, M. Rafiq, S. A. Mohd Yatim, A. Ahmad, M. Irfan & M. S. Ehsan, "Mathematical modeling for transmission dynamics of hepatitis B virus", Punjab University Journal of Mathematics **57** (2025) 964. https://doi.org/10.52280/19zged66.
[17] S. Zeb, S. A. Mohd Yatim, A. Kamran, S. Zulfiqar, M. Rafiq & N. Mohamad Noor, "A nonlinear delay mathematical model for predicting chlamydia dynamics and intervention effects", Communication in Biomathematical Sciences **8** (2025) 132. https://doi.org/10.5614/cbms.2025.8.2.1.
[18] H. Waaler, A. Geser & S. Andersen, "The use of mathematical models in the study of the epidemiology of tuberculosis", American Journal of Public Health and the Nations Health **52** (1962) 1002. https://pmc.ncbi.nlm.nih.gov/articles/PMC1523050/.
[19] C. S. Revelle, W. R. Lynn & F. Feldmann, "Mathematical models for the economic allocation of tuberculosis control activities in developing nations", American review of respiratory disease **96** (1967) 893. https://pubmed.ncbi.nlm.nih.gov/6059199/.
[20] C. Castillo-Chavez & Z. Feng, Mathematical models for the disease dynamics of tuberculosis, 1996. https://www.researchgate.net/publication/216082926_Mathematical_models_for_the_disease_dynamics_of_tuberculosis#full-text.
[21] Y. Yang, J. Li, Z. Ma & L. Liu, "Global stability of two models with incomplete treatment for tuberculosis", Chaos, Solitons & Fractals **43** (2010) 79. https://doi.org/10.1016/j.chaos.2010.09.002.
[22] J. M. Trauer, J. T. Denholm & E. S. McBryde, "Construction of a mathematical model for tuberculosis transmission in highly endemic regions of the Asia-Pacific", Journal of Theoretical Biology **358** (2014) 74. https://doi.org/10.1016/j.jtbi.2014.05.023.
[23] J. Zhang, Y. Li & X. Zhang, "Mathematical modeling of tuberculosis data of china", Journal of Theoretical Biology **365** (2015) 159. https://doi.org/10.1016/j.jtbi.2014.10.019.
[24] S. Kim, A. A. V. de los Reyes & E. Jung, "Mathematical model and intervention strategies for mitigating tuberculosis in the Philippines", Journal of Theoretical Biology **443** (2018) 100. https://doi.org/10.1016/j.jtbi.2018.01.026.
[25] E. Jung, S. Lenhart & Z. Feng, "Optimal control of treatments in a two-strain tuberculosis model", Discrete and Continuous Dynamical Systems Series B **2** (2002) 473. https://www.math.purdue.edu/~fengz/documents/publications/jlf.pdf.
[26] S. Whang, S. Choi & E. Jung, "A dynamic model for tuberculosis transmission and optimal treatment strategies in South Korea", Journal of Theoretical Biology **279** (2011) 120. https://doi.org/10.1016/j.jtbi.2011.03.009.
[27] S. Choi, E. Jung & S.-M. Lee, "Optimal intervention strategy for prevention tuberculosis using a smoking-tuberculosis model", Journal of Theoretical Biology **380** (2015) 256. https://doi.org/10.1016/j.jtbi.2015.05.022.
[28] K. J. B. Villasin, A. R. Lao & E. M. Rodriguez, "A dynamical analysis of tuberculosis in the philippines", Philipp Sci Lett **10** (2017) 29. https://scienggj.org/2017/PSL%202017-vol10-no01-p29-37%20Rodriguez.pdf.
[29] J. Liu & T. Zhang, "Global stability for a tuberculosis model", Mathematical and Computer Modelling **54** (2011) 836. https://doi.org/10.1016/j.mcm.2011.03.033.
[30] D. Okuonghae, "A mathematical model of tuberculosis transmission with heterogeneity in disease susceptibility and progression under a treatment regime for infectious cases", Applied Mathematical Modelling **37** (2013) 6786. https://doi.org/10.1016/j.apm.2013.01.039.
[31] A. O. Egonmwan & D. Okuonghae, "Analysis of a mathematical model for tuberculosis with diagnosis", Journal of Applied Mathematics and Computing **59** (2018) 129. https://doi.org/10.1007/s12190-018-1172-1.
[32] M. Caputo & M. Fabrizio, "A new definition of fractional derivative without singular kernel", Progress in fractional differentiation & applications **1** (2015) 73. https://www.naturalspublishing.com/files/published/0gb83k287mo759.pdf.
[33] T. Akman Yildiz, A. Jajarmi, B. Yildiz & D. Baleanu, "New aspects of time fractional optimal control problems within operators with nonsingular kernel", Discrete and Continuous Dynamical Systems **13** (2020) 407. https://doi.org/10.3934/dcdss.2020023.

[34] A. Atangana & D. Baleanu, "New fractional derivatives with nonlocal and non-singular kernel: theory and application to heat transfer model (Version 1)", arXiv (2016). https://doi.org/10.48550/ARXIV.1602.03408.
[35] A. Akgul, "A novel method for a fractional derivative with non-local and non-singular kernel", Chaos, Solitons & Fractals **114** (2018) 478. https://doi.org/10.1016/j.chaos.2018.07.032.
[36] S. C. Brailsford, P. R. Harper, B. Patel & M. Pitt, "An analysis of the academic literature on simulation and modelling in health care", Journal of Simulation **3** (2009) 130. https://doi.org/10.1057/jos.2009.10.
[37] R. K. Alhefthi, M. A. ur Rehman, N. Ahmed, Z. Iqbal, M. Inc, M. Iqbal, M. S. Iqbal, A. Raza & M. Rafiq, "Developing a computational framework for accurately solving a mathematical model of streptococcus pneumonia infection", Biomedical Signal Processing and Control **103** (2025) 107427. https://doi.org/10.1016/j.bspc.2024.107427.
[38] S. Salim, F. Dayan, M. A. U. Rehman & H. A. Neamah, "Optimization and control in rubella transmission dynamics: a boundedness-preserving numerical model with vaccination", Informatics in Medicine Unlocked **51** (2024) 101595. https://doi.org/10.1016/j.imu.2024.101595.
[39] M. Yavuz, F. Ozkose, M. Akman & Z. T. Tastan, "A new mathematical model for tuberculosis epidemic under the consciousness effect", Mathematical Modelling and Control **3** (2023) 88. https://doi.org/10.3934/mmc.2023009.
[40] A. Akgul, M. Sajid Iqbal, U. Fatima, N. Ahmed, Z. Iqbal, A. Raza, M. Rafiq & M. A. Rehman, "Optimal existence of fractional order computer virus epidemic model and numerical simulations", Mathematical Methods in the Applied Sciences **44** (2021) 10673. https://doi.org/10.1002/mma.7437.
[41] A. Ahmad, M. Uzair Awan, S. Zeb, B. Ceesay, M. Rafiq, A. Kamran & A. Shaukat, "A delay mathematical model to examine control strategies of the coronavirus pandemic with an efficient approach", Advances in Differential Equations and Control Processes, **32** (2025), 3703. https://doi.org/10.59400/adecp3703.
[42] S. Zeb, S. A. Mohd Yatim, A. Kamran, M. Rafiq & Y. Wee Ping, "A review of Malaysian epidemiological dengue control models data and future directions for sustainable dengue management", Journal of Sustainability Science and Management **21** (2026) 984. https://doi.org/10.46754/jssm.2026.04.012.